2015

Apolipoprotein D modulates amyloid pathology in APP/PS1 Alzheimer's disease mice

Hongyun Li
University of Wollongong, hongyun@uow.edu.au

Kalani R. Ruberu
University of Wollongong, kalani@uow.edu.au

Sonia Sanz Munoz
University of Wollongong, ssm886@uowmail.edu.au

Andrew M. Jenner
University of Wollongong, ajenner@uow.edu.au

Adena S. Spiro
University of Wollongong, adena@uow.edu.au

See next page for additional authors

Publication Details

Li, H., Ruberu, K., Sanz Munoz, S., Jenner, A. M., Spiro, A., Zhao, H., Rassart, E., Sanchez, D., Ganfornina, M. D., Karl, T. & Garner, B. (2015). Apolipoprotein D modulates amyloid pathology in APP/PS1 Alzheimer's disease mice. Neurobiology of Aging, 36 (5), 1820-1833.

Apolipoprotein D modulates amyloid pathology in APP/PS1 Alzheimer's disease mice

Abstract

Apolipoprotein D (apoD) is expressed in the brain and levels are increased in affected brain regions in Alzheimer's disease (AD). The role that apoD may play in regulating AD pathology has not been addressed. Here, we crossed both apoD-null mice and Thy-1 human apoD transgenic mice with APP-PS1 amyloidogenic AD mice. Loss of apoD resulted in a nearly 2-fold increase in hippocampal amyloid plaque load, as assessed by immunohistochemical staining. Conversely, transgenic expression of neuronal apoD reduced hippocampal plaque load by approximately 35%. This latter finding was associated with a 60% decrease in amyloid β 1-40 peptide levels, and a 34% decrease in insoluble amyloid β 1-42 peptide. Assessment of β-site amyloid precursor protein cleaving enzyme-1 (BACE1) levels and proteolytic products of amyloid precursor protein and neuregulin-1 point toward a possible association of altered BACE1 activity in association with altered apoD levels. In conclusion, the current studies provide clear evidence that apoD regulates amyloid plaque pathology in a mouse model of AD.

Disciplines

Medicine and Health Sciences

Publication Details

Li, H., Ruberu, K., Sanz Munoz, S., Jenner, A. M., Spiro, A., Zhao, H., Rassart, E., Sanchez, D., Ganfornina, M. D., Karl, T. & Garner, B. (2015). Apolipoprotein D modulates amyloid pathology in APP/PS1 Alzheimer's disease mice. Neurobiology of Aging, 36 (5), 1820-1833.

Authors

Hongyun Li, Kalani R. Ruberu, Sonia Sanz Munoz, Andrew M. Jenner, Adena S. Spiro, Hua Zhao, Eric Rassart, Diego Sanchez, Maria D. Ganfornina, Tim Karl, and Brett Garner

Apolipoprotein-D modulates amyloid pathology in APP/PS1 Alzheimer's disease mice

Hongyun Li[a,b], Kalani Ruberu[a,b], Sonia Sanz Muñoz[a,b], Andrew M. Jenner[a,b], Adena Spiro[a,b], Hua Zhao[a,b], Eric Rassart[c,d], Diego Sanchez[e], Maria D. Ganfornina[e], Tim Karl[f,g,h] and Brett Garner[a,b,*]

[a] Illawarra Health and Medical Research Institute, University of Wollongong, NSW 2522, Australia; [b] School of Biological Sciences, University of Wollongong, NSW 2522, Australia; [c] Laboratoire de biologie moléculaire, Département des Sciences Biologiques, and [d] BioMed, centre de recherches biomédicales, Université du Québec à Montréal, Case Postale 8888 Succ. Centre-ville, Montréal, H3C 3P8, Canada; [e] Departamento de Bioquímica y Biología Molecular y Fisiología - Instituto de Biología y Genética Molecular, Universidad de Valladolid - CSIC, Valladolid, Spain; [f] Neuroscience Research Australia, Randwick NSW 2031, Australia; [g] School of Medical Sciences, University of New South Wales, NSW 2052, Australia; [h] Schizophrenia Research Institute, Darlinghurst NSW 2010, Australia.

[*] Corresponding author at: School of Biological Sciences, University of Wollongong, NSW 2522, Australia. Tel.: +61-2-4298 1576, Fax. +61-2-4221 8130, Email: brettg@uow.edu.au

ABSTRACT

Apolipoprotein-D (apoD) is expressed in the brain and levels are increased in affected brain regions in Alzheimer's disease (AD). The role that apoD may play in regulating AD pathology has not been addressed. Here we crossed both apoD null mice and Thy-1 human apoD transgenic mice with APP-PS1 amyloidogenic AD mice. Loss of apoD resulted in an ~ 2-fold increase in hippocampal amyloid plaque load assessed by immunohistochemical staining. Conversely, transgenic expression of neuronal apoD reduced hippocampal plaque load by ~ 35%. This latter finding was associated with a 60% decrease in amyloid-beta 1-40 peptide levels, and a 34% decrease in insoluble amyloid-beta 1-42 peptide. Assessment of beta-site amyloid precursor protein cleaving enzyme-1 (BACE1) levels and proteolytic products of amyloid precursor protein and neuregulin-1 point towards a possible association of altered BACE1 activity in association with altered apoD levels. In conclusion, the current studies provide clear evidence that apoD regulates amyloid plaque pathology in a mouse model of AD.

Keywords: Apolipoprotein-D, Alzheimer's disease, amyloid-pathology, amyloid-β, neurodegeneration.

Abbreviations: Aβ, amyloid-beta peptide; AD, Alzheimer's disease; apoD, apolipoprotein-D; BACE1, beta-site amyloid precursor protein cleaving enzyme-1; BCA, bicinchoninic acid; BHT, butylated hydroxytoluene; CTFs, C-terminal fragments; DKO, apoD gene knockout mice; DTG, human apoD transgenic mice; L-OOH, lipid hydroperoxide; MTBE, Methyl-*tert*-butyl ether; ThS, thioflavine S

1. Introduction

ApoD is expressed in the brain and levels are increased during brain development and aging (Kim et al., 2009). It is also established that apoD levels are increased in affected brain regions in Alzheimer's disease (AD) and in AD mouse models (Bhatia et al., 2013; Terrisse et al., 1998; Thomas et al., 2003; Thomas et al., 2001). Additional studies show that brain lipid peroxidation is increased during aging (Cristiano et al., 1995; Droge and Schipper, 2007), as well as in AD and AD mouse models (Abdul et al., 2008; Markesbery and Carney, 1999; Montine et al., 2007; Sayre et al., 1997; Schuessel et al., 2005). Furthermore, recent studies show that the increase in apoD associated with aging and AD in human brain tissues is correlated with markers of lipid oxidative stress (Bhatia et al., 2013; Kim et al., 2009). These findings are particularly pertinent as a novel role for apoD in the control of brain lipid peroxidation has been reported (Bajo-Graneras et al., 2011; Bajo-Graneras et al., 2011; Ganfornina et al., 2008). Studies in mice revealed that brain apoD is induced in response to oxidative stress, that lipid peroxidation is increased in the brains of apoD null mice, and that neuronal expression of human apoD prevents brain lipid peroxidation in response to paraquat-induced oxidative stress (Ganfornina et al., 2008).

One mechanism by which apoD acts as a lipid antioxidant involves the interaction of a single conserved Met residue located within the hydrophobic patch at the entrance of the apoD ligand binding pocket (Bhatia et al., 2012; Oakley et al., 2012). The apoD Met_{93} residue interacts directly with potentially reactive radical-generating lipid hydroperoxide (L-OOH) species, converting them to non-reactive lipid hydroxides, an antioxidant activity that is lost when Met_{93} is replaced with Ala (Bhatia et al., 2012). One consequence of this reaction is the

formation of a Met-sulfoxide residue that destabilizes the protein and promotes its non-covalent dimerization (Bhatia et al., 2012). Interestingly, apoD dimers have been identified in the hippocampus, but not in the pathologically spared cerebellum, of human AD subjects (Bhatia et al., 2013). There is now a growing consensus that apoD may play a protective role in AD, and other neurological diseases (Bhatia et al., 2013; Dassati et al., 2014).

One important question that remains unanswered centres on the postulated protective function of apoD in AD and whether it could modulate pathological processes (including those associated with amyloid plaque pathology and lipid peroxidation) or simply represent a marker of disease progression. Based on the studies cited above, we hypothesized that apoD gene deletion may exacerbate the AD phenotype in amyloidogenic AD mice whereas early over-expression of apoD in neurons would have the opposite effect, and reduce the AD amyloidogenic phenotype. In the current study we have addressed this hypothesis by crossing apoD null mice, as well as transgenic mice expressing human apoD in neurons, with APP/PS1 amyloidogenic mice and assessing for possible alterations in amyloid plaque load and markers of brain lipid peroxidation.

2. Materials and Methods

2.1. Materials

Methyl-*tert*-butyl ether (MTBE), chloroform and methanol were HPLC grade and purchased from Thermo Scientific, Scoresby, VIC, Australia. Analytical grade ammonium acetate was from Crown Scientific, Moorebank, NSW, Australia. Screw thread vials (4 mL) and wide

mouth vials (1.8 mL) with PTFE/silicone septa caps were from Grace Davison, Rowville, VIC, Australia. The internal lipid standard mixture contained AA (Avanti Polar Lipids purchased from Auspep, Tullamarine, VIC, Australia) and F_2-isoprostanes in chloroform/methanol (2:1, vol:vol). F_2-isoprostanes $F_2\alpha$III-ISP (8-*iso*-prostaglandin $F_2\alpha$) and $F_2\alpha$VI-ISP (5*S*,9α,11α,-trihydroxy-1α,1β,1γ-trihomo-18,19,20-trinor-8β-prosta-2Z,6E-dien-1-oic acid) were purchased from Cayman Chemicals (Ann Arbor, MI, USA). Other reagents including analytical grade butylated hydroxytoluene (BHT) and sodium hydroxide (98% minimum) were from Sigma Aldrich, Sydney, NSW, Australia.

2.2. Transgenic mice

Three strains of mice were used to generate amyloidogenic AD mice with either increased neuronal expression of apoD or a complete lack of apoD. We used the APP-PS1 AD mouse model expressing chimeric mouse/human APP695swe/Swedish mutations (K595N/M596L) and mutant human PS1 (PS1/ΔE9) obtained from the Jackson Laboratory (Bar Harbor, USA; Strain name, B6.Cg-Tg AβPPswePSEN1dE9)85Dbo/J; Stock #005864) and maintained as double hemizygotes on a C57BL/6J background as described previously (Cheng et al., 2013; Jankowsky et al., 2004). This AD mouse model is on a pure (backcrossed > 10 generations) C57BL6 background and has well characterised plaque pathology (Garcia-Alloza et al., 2006). These mice have a pronounced AD phenotype with amyloid deposits by 6 months of age which is accompanied by neuron loss and hippocampal atrophy by 12 months (Garcia-Alloza et al., 2006). The generation and characterisation of the apoD gene knockout (DKO) mice and the human apoD transgenic (DTG) mice (DTG mice selectively expresses human apoD in neurons under the control of the Thy-1 promoter) was previously described (Ganfornina et al., 2008). The neuron-specific expression of human apoD in the DTG mice

has been established (Do Carmo et al., 2008; Ganfornina et al., 2008). Hemizygous APP-PS1 mice were crossed with either DKO or DTG mice to generate APP-PS1/DKO$^{+/-}$ and APP-PS1/DTG$^{+/-}$ breeders. These mice were used to generate APP-PS1/DKO$^{+/+}$ and APP-PS1/DTG$^{+/+}$ and littermate APP-PS1 control groups. As previously described (Jankowsky et al., 2004), the expression of the human mutant AβPPswe and PSEN1dE9 segregate together. All test animals were hemizygous with respect to the AβPPswe and PSEN1dE9 transgenes, in line with standard protocols for amyloidogenic AD mouse models (Gotz and Ittner, 2008; Higgins and Jacobsen, 2003). All mice were on a pure (backcrossed > 10 generations) C57BL6 background. Genotyping of the APP-PS1, DKO and DTG mice has been described previously (Ganfornina et al., 2008; Kim et al., 2010). Test animals were females at ~11 months of age (DKO Study: APP-PS1, n = 9, 49.7 ± 4.7 weeks old; APP-PS1/DKO n = 7, 50.7 ± 4.3 weeks old; DTG Study: APP-PS1, n = 8, 44.2 ± 1.6 weeks old; APP-PS1/DTG n = 7, 44.2 ± 2.1 days old). Female APP-PS1 mice were used as they accumulate a more sever amyloid pathology at an early age compared to male APP-PS1 mice (Wang et al., 2003). Ethics approval was from the University of Wollongong and the University of New South Wales animal ethics committees.

2.3. Tissue preparation

Mice were euthanized by CO_2 asphyxiation and transcardially perfused with ice-cold phosphate buffered saline (PBS). The brains were removed and sagittally divided and the hippocampus dissected from the right hemisphere before snap freezing and storage at -80˚C. The left hemisphere was immersion fixed in 4% paraformaldehyde in 0.1 M phosphate buffer (PB) at 4˚C for three days, then preserved in 30% (w/v) sucrose in 0.1M PB with 0.01% sodium azide at 4˚C until sectioning. Six sets of 45 μm sagittal cryo-sections were collected

and stored at -20˚C in antifreeze solution for histological and immunohistochemiical analysis. One part of pulverized hippocampus (~15mg) was homogenized in 10 volumes of 140 mM NaCl, 3 mM KCl, 25 mM Tris (pH 7.4), containing 1% Nonidet P-40 and Roche complete protease inhibitors (TBS/NP40 extraction buffer) using a Precellys 24 homogenizer (2 x 30s, 6000 *g*). Homogenates were centrifuged at 20,817 *g* for 15 min at 4˚C and the TBS/NP40-soluble supernatant aliquoted into several tubes and stored at −80˚C until use in western blotting and ELISA experiments. Protein concentration was measured using the bicinchoninic acid (BCA) method.

2.4. PCR

Mouse genotyping was assessed on DNA extracted from tail tips using the ISOLATE Genomic DNA mini kit (BIO-52032, Bioline Sydney, Australia) as described previously (Borchelt et al., 1996; Do Carmo et al., 2009; Ganfornina et al., 2008). For brain mRNA analysis, total RNA from the cortex was extracted using TriReagent and RNA concentrations determined using a Nanodrop 1000 spectrophotometer (Thermo Fisher Scientific) and 260/230 nm and 260/280 nm absorbance ratios used to determine RNA purity. Two μg of total RNA was used for reverse transcription with oligo dT(18) primers using the Tetro cDNA Synthesis kit (Bioline, Sydney, Australia). For apoD mRNA validation, PCR was conducted on an Eppendorf Master cycler or a Bio-Rad Thermalcycler using My Taq HS Mix (Bioline, Sydney, Australia) with the following primer pairs: human apoD: forward, 5' - TGC AGG AGA ATT TTG ACG TG - 3', reverse, 5' - AGG TTA ACT GGG GTG GCT TC - 3'; mouse apoD: forward, 5' - CCA CCG GCA CCC TAC TGG ATC - 3', reverse, 5' - CGG GCA GTT CGC TTG ATC TGT - 3'. The PCR amplicons separated in 2% agarose gels were visualized using by Gel Logic 212 Pro image system (Carestream Health, Inc. NY, USA).

Mouse apoE mRNA analysis was carried out in a Roche Lightcycler 480 real-time PCR system using SensiFAST SYBR No-ROX kit (Bioline, Sydney, Australia), following the manufacturer's protocol with primer pairs: forward, 5'- AAC AGA CCC AGC AAA TAC GCC - 3', reverse, 5' - CTC ATT GAT TCT CCT GGG CC - 3'. The level of apoE expression was calculated using the comparative threshold cycle (Ct) value method using the formula $2^{-\Delta\Delta Ct}$.

2.5. Aβ ELISA

Aβ40 and Aβ42 in TBS/NP40-soluble hippocampal homogenates were quantified using ELISA kits (Cat #SIG-38954 and SIG-38956, Covance, North Ryde NSW, Australia or EZBRAIN-SET, EMD Millipore Corporation, Billerica, MA, USA) following the manufacturer's instructions as described (Kim et al., 2013). The insoluble hippocampal homogenate fractions were prepared by centrifugation of TBS/NP40-soluble hippocampal homogenates at 20,817 x *g* for 15 min at 4°C and the pellet was homogenized with 6 volumes of 6.25 M guanidine HCl (gHCl) and assayed by ELISA, as previously described in detail (Kim et al., 2013), to give an estimate of "insoluble" Aβ 40 and Aβ 42 levels in the hippocampus. Samples were diluted 1:10 ($A\beta_{40}$) or 1:50 ($A\beta_{42}$) and assayed in duplicate. Aβ40 and Aβ42 levels in extracts were calculated by comparing samples to the Aβ standard curves.

2.6. Plaque histology

Staining of hippocampal tissues with thioflavine S (ThS) and anti-Aβ monoclonal antibody 6E10 was performed as described previously (Kim et al., 2013). In brief, sagittal sections (45

μm thick, free floating) were rinsed extensively with TBS to remove cryo-protectants and immersed in distilled H_2O (2 min), Harris hematoxylin (2 min), distilled H_2O (3 min), 1% (w/v) ThS (Sigma T1892, 3 min), distilled H_2O (3 min), 1% (v/v) acetic acid (20 min), distilled H_2O (3 min), and mounted in buffered glycerol. Three sections per mouse were analysed from the cortical and hippocampal regions between lateral 1 mm to lateral 2 mm from the midline as defined using a mouse brain atlas (Franklin and Paxinos, 2007). Images were captured using a Nikon TE2000 microscope equipped with a SPOT digital camera (Diagnostic Instruments) and Image-Pro Plus 6.1 software (Media Cybernetics, Silver Spring MD, USA). Hippocampal ThS-positive plaque load was quantified as percentage coverage of the area of interest (measured as μm^2) using ImageJ. Data are presented as relative values compared to the relevant control group (which was arbitrarily assigned a value of 1.0).

For amyloid plaque immunohistochemistry, sections were pre-treated with 95% formic acid for 5 minutes, rinsed with tap water, then quenched with 1% H_2O_2 for 30 min. After blocking, sections were incubated with biotin-6E10 monoclonal antibody (1:5000, Cat# SIG-39340, Covance,), for 16 h at 4˚C, followed by streptavidin-HRP (Sigma,S2438, 1:4000), 1 h at 22˚C. The sections were developed using DAB substrate (SK-4105, Vector Laboratories) and scanned at 20X magnification (Aperio Digital Pathology System, Aperio Technologies). The percentage of the area occupied by immunoreactive products above background staining was measured in the hippocampal region (three sections per mouse, between lateral 1 mm to lateral 2.5 mm from the midline) using ImageJ software. Data are presented as relative values compared to the relevant control group (which was arbitrarily assigned a value of 1.0).

2.7. Immunohistochemistry methods for apoD, BACE1, GFAP and Iba1 staining

After removal of cryo-protectants, consecutivesetsofsagittalsections(45μmthick)fromthe different mouse groups were immunostained for BACE1, GFAP and Iba1 with the peroxidase-3,3′-diaminobenzidine (DAB) method as previously described for immunohistochemistry (Kim et al., 2013). Briefly, sections were treated with 1% H_2O_2 in PBS for 30 minutes after antigen retrieval by boiling the sections in citrate buffer (0.01M, pH 6.0 for 5min). Sections were then pre-incubated in 5% horse serum in PBS with 0.5% Triton X-100 for 1 h, and then incubated withtheprimaryantibodiesat4˚C overnight (BACE1 1:400, rabbit monoclonal, Cat# 5606, Cell Signalling; GFAP, 1:2000, rabbit polyclonal Cat# Z0334, DAKO; Iba1, 1:2000, rabbit polyclonal, Cat# 019-19741, Wako). Sections were further reacted with a biotinylated pan-specific secondary antibody (goat anti-rabbit IgG, Cat# B7398, Sigma) at 1:200 for 2 h, and subsequently with Streptavidin−Peroxidase Polymer (1:5000, Sigma Cat# S2438) for 1 h. Immunoreaction product was visualized in SIGMAFAST™DAB with Metal Enhancer (Cat# D0426). The mounted slides were scanned at 20X magnification with Aperio Digital Pathology System (Aperio Technologies, USA).

The methods used for apoD immunofluorescence detection were as described previously (Lagares et al., 2007; Li et al., 2007). In brief, free-floating sagittal brain sections from WT, APP-PS1, APP-PS1/DTG mice were probed using an antibody raised against human apoD (1:400, clone EPR2916, rabbit monoclonal Cat# Ab108191, Abcam) alone, or with anti-NeuN (1:500, Clone A60, mouse monoclonal Cat# MAB377, EMD-Millipore) double-staining to localize apoD in neurons. Another set of sections from APP-PS1/DKO mice were used for double-labelling with an Aβ antibody (WO2 hybridoma culture media, 1:50, gift or Dr Qiao-Xin Li and Prof Colin Masters, University of Melbourne). Where indicated, the additional antibodies (BACE1 1:500, GFAP 1:2000, Iba1 1:1000) were also included. Donkey anti-rabbit Alexa flour 488 (1:250, Cat# A-21206, Life Technologies) and donkey

anti-mouse IgG conjugated Alexa flour-594 (1:500, Cat# A-21203, Life Technologies) were used as the secondary antibodies. After mounting with anti-fade media (Cat#10981, Sigma), coverslips were sealed with nail polish, and the samples were stored at 4˚C. Images were captured using 4X and 10X objective lens (with an ocular lens at 10X) in a Nikon TE2000 microscope equipped with a SPOT digital camera (Diagnostic Instruments) and Image-Pro Plus 6.1 software (Media Cybernetics, Silver Sprin MD, USA). High-power images were taken using a Leica TCS SP5 confocal laser-scanning microscope (Leica Microsystems, Germany). Optical density in the area of interest was measured using ImageJ (http://rsb.info.nih.gov/ij/) as described previously (Kim et al., 2013), using freehand selection to outline hippocampal and cortical regions (sampling section immunolabelling tools). Data were compared to appropriate control mouse groups for both the DKO and DTG groups and statistical differences were assessed using the student's t-test where $P < 0.05$ was considered significant.

2.8. Western blotting

TBS/NP40-soluble homogenates were analysed by SDS-PAGE (~15 to 50 μg protein per lane) and western blotting using antibodies to: apoD (sc-34760 or sc-166612, Santa Cruz, 1:5000), apoE (Cat# 178479, Merck Millipore, 1:5,000), APP (WO2 monoclonal provided by Dr Qiao-Xin Li and Prof Colin Masters, University of Melbourne, 1:200), APP C-terminal fragments (A8717, Sigma, 1:10,000), BACE1 (Ab108392, clone EPR3956, Abcam, 1:5,000) NRG-1 C-terminal fragments (SC-348, Santa Cruz, 1:500), HNE (recognizes proteins modified by the aldehydic lipid peroxidation end product, 4-hydroxynonenal) (MAB3248, R&D Systems, 1:2,000) and β-actin (A5060, Sigma, 1:10,000). Signals were detected using species-specific HRP-conjugated secondary antibodies (Dako) and enhanced

chemiluminescence and quantified using ImageJ software. Integrated optical density data were normalized to β-actin levels and expressed as relative values.

2.9. Analysis of F_2-isoprostanes by GC-MS

Lipid extracts (from ~5 mg tissue) were hydrolysed overnight for GC-MS analysis of F_2-isoprostanes as described previously (Abbott et al., 2013). Samples were loaded onto pre-conditioned solid phase extraction columns (UCT CUQAX223 3 ml; United Chemical Technologies, Bristol, USA) and washed with 2ml of 40 mM formic acid (pH 4.5) containing 40% (v/v) methanol and 2ml hexane/MTBE (1:1). F_2-isoprostanes and fatty acids were eluted from the SPE columns with MTBE containing 20% methanol and 1% formic acid. The F_2-isoprostane and fatty acid fraction was dried down under nitrogen and derivatised with 30 µl of pentafluorobenzylbromide (PFBBr) (10% in acetonitrile) and 15 µl of N,N-diisopropylethylamine (DIPEA) (10% in acetonitrile) at 37°C for 30 min. Excess reagents were evaporated under nitrogen. The F_2-isoprostane PFBenzyl ester was derivatised with 20 µl acetonitrile plus 20 µl BSTFA+1% TMCS for 1 hour at 37°C. The derivatised samples were dried under nitrogen, reconstituted in 40 µl toluene and analysed using an Agilent 7000B triple quadrupole mass selective detector interfaced with an Agilent 7890A GC system gas chromatograph, equipped with an automatic sampler and a computer workstation. Selected-reaction monitoring (SRM) was performed using the negative chemical ionisation (NCI) mode (70eV) with argon as the reagent gas (1.25 ml/min) and the collision gas (0.6 ml/min). The ion source was maintained at 150°C and the quadrupoles at 150°C. For F_2-isoprostane analysis, derivatised samples (1 µl) were injected splitless into the GC injection port. Column temperature was increased from 180°C to 280°C, at 40°C/min, then to 292°C, at 2°C/min, and finally to 305°C, at 50°C/min, with a final hold of 4 min. Quantification of

F_2-isoprostanes ($F_2\alpha$III-ISP + $F_2\alpha$VI-ISP) was achieved by comparison of specific SRM transitions with their corresponding heavy isotope internal standards. Relative molar response factors for each analyte were calculated from calibration curves constructed from different concentrations in triplicate, AA and DHA (1 to 25 μg) and F_2-isoprostanes (0.25 – 2.5 ng), and showed good linearity ($r^2 > 0.98$).

2.10. Data analysis

Quantitative data are presented as mean ± SE (represented by the error bars) from 7 to 9 mice unless stated otherwise. Statistical differences were assessed using the student's t-test where $P < 0.05$ was considered significant.

3. Results

3.1. Generation of APP-PS1 mice that lack apoD or express human apoD in neurons

We crossed APP-PS1 mice with both apoD knockout (DKO) and human apoD overexpressing transgenic (DTG) mice to assess the impact this may have on the amyloid phenotype of this AD mouse model. Analysis of murine apoD using PCR methods confirmed the absence of apoD mRNA in the brain of APP-PS1/DKO mice (Fig. 1A). The presence of human apoD mRNA was similarly confirmed by PCR to be present only in the APP-PS1/DTG line (Fig. 1B). The loss of apoD protein was confirmed the APP-PS1/DKO mice (Fig. 1C). As previous studies have suggested there may be compensatory changes between apoE and apoD in mice (Terrisse et al., 1999) and humans (Kim et al., 2009), possibly due to a partial overlap in lipid-binding functions, we also assessed apoE protein levels. ApoD

deletion did not significantly alter apoE protein levels, although we did observe a trend ($p = 0.06$) for 14% lower apoE in the APP-PS1/DKO mice (Fig. 1C and 1E). Further analysis of apoE mRNA indicated there was no change associated with apoD loss (Fig. 1F).

Regarding the APP-PS1/DTG mice, previous studies have confirmed the neuron-specific expression of human apoD (under the control of the Thy-1 promoter) in these mice (Do Carmo et al., 2008; Ganfornina et al., 2008). This is a valid model for the study of neurological disease as even though the vast majority of apoD in the brain is expressed by glial cells, under pathological conditions apoD is also detected in neuronal populations (Desai et al., 2005; Elliott et al., 2010; Kalman et al., 2000; Rassart et al., 2000). We used an antibody that cross-reacts with both mouse and human apoD in order to assess any possible change in global apoD levels in APP-PS1/DTG mice. The neuronal expression of human apoD resulted in a modest but statistically significant increase (by 20%) in total apoD protein levels (Fig. 1D and 1E). Although the presence of apoD in neurons from human apoD transgenic DTG mice has been previously demonstrated (Do Carmo et al., 2008; Ganfornina et al., 2008) (and O. Najyb and E. Rassart, unpublished data), we also confirmed this in the present studies using immunohistochemical techniques. These experiments confirmed that neuronal apoD was increased in the APP-PS1/DTG mice compared to the APP-PS1 control mice (Fig. 2). Analysis of the apoD staining indicated the majority of the apoD was neuronal (although non-neuronal staining was also detected, arrows Fig. 2G-I). Quantitative analysis of apoD staining indicated a significant overall increase in apoD levels of 21% in the APP-PS1/DTG mice compared to the APP-PS1 control mice (Fig. 2J). It is noteworthy that endogenous mouse apoD levels were also higher in the APP-PS1 mice as compared to wild type C57Bl6J mice (Fig. 2J). The total increase in apoD levels in the APP-PS1/DTG

therefore reflects up-regulation of endogenous mouse apoD (in agreement with previous studies, (Thomas et al., 2001)) and human apoD resulting from transgenic expression.

Neither apoE protein (Fig. 1D and 1E) nor apoE mRNA (Fig. 1F) was altered in the APP-PS1/DTG mice compared to control APP-PS1 mice. The APP-PS1/DKO and APP-PS1/DTG mice we generated therefore represented an appropriate model to probe for apoD-related changes in amyloid pathology that are free of any confounding influences associated with altered apoE levels.

3.2. Deletion of apoD significantly increases amyloid plaque pathology in APP-PS1 mice

The extent of cortical Aβ deposition was assessed in sagittal sections from 11-month-old APP-PS1 and APP-PS1/DKO mice using both 6E10 and ThS staining as quantitative markers of plaque pathology. Immunohistochemical staining demonstrated numerous 6E10 positive plaques in the hippocampus and cortex of APP-PS1 mice (Fig. 3A). Hippocampal 6E10 plaque pathology was approximately doubled in the APP-PS1/DKO mice compared to the APP-PS1 mice (Fig. 3A and 3C). ThS staining was also used as an additional marker of amyloid plaque load. ThS binds to β-sheet rich structures including components of both amyloid plaques and neurofibrillary tangles. ThS staining confirmed that hippocampal plaque pathology was significantly increased in the APP-PS1/DKO mice compared to the APP-PS1 control mice (Fig. 3B and 3C). Very similar increases in amyloid plaque and ThS staining were also detected in the cortex of APP-PS1/DKO as compared to the control APP-PS1 mice (Fig. 3D).

We also used an ELISA method to assess hippocampal levels of soluble $A\beta_{40}$ and $A\beta_{42}$ in both APP-PS1 mice and APP-PS1/DKO mice. Despite the increase in plaque pathology noted above, levels of soluble $A\beta_{40}$ and $A\beta_{42}$ were not significantly changed by the loss of apoD in APP-PS1 mice (Fig. 4A). The pellets from the soluble homogenate fractions were also dissolved in gHCl and assessed by ELISA to give an indicator of "insoluble"$A\beta_{40}$ and$A\beta_{42}$ levels. Although a trend for increased levels of $A\beta_{40}$ was noted (Fig. 4C), this was not statistically significant. Overall, these data indicate that the deletion of apoD in APP-PS1 mice results in a significant increase in hippocampal amyloid plaque pathology.

3.3. Neuronal expression of human apoD significantly decreases amyloid plaque pathology in APP-PS1 mice

Using the same suite of techniques utilised in the analysis of plaque pathology in APP-PS1/DKO mice, a parallel study focusing on neuronal expression of human apoD in the APP-PS1/DTG mice was conducted. In contrast to results arising from apoD deletion, neuronal expression of human apoD led to a significant reduction in hippocampal and cortical amyloid plaque pathology as assessed by both 6E10 and ThS staining of the APP-PS1/DTG brain sagittal sections compared to control APP-PS1 tissues (Fig. 5A-D). Furthermore, levels of soluble $A\beta_{40}$ in the APP-PS1/DTG hippocampus were reduced to less than half the level detected in control APP-PS1 mice (Fig. 4B) and there was a trend ($p = 0.077$) for a similar reduction in the insoluble$A\beta_{40}$ in the same group comparison (Fig 4D). Interestingly, levels of insoluble (but not soluble) $A\beta_{42}$ were significantly reduced (by 34%) in the APP-PS1/DTG mice compared to control APP-PS1 mice (Fig. 4D). The reasons for the selective effect of apoD overexpression on different Aβ species is not entirely clear. Of potential relevance, it is known hat the ratio of Aβ 42:Aβ 40 changes dramatically depending on the stage of amyloid

pathology in APP-PS1 mice (Wang et al., 2003). Overall, these data indicate that neuronal expression of human apoD significantly decreases hippocampal amyloid plaque pathology in APP-PS1 mice.

3.4. Impact of apoD modulation on APP processing

Based on the significant changes in amyloid plaque load detected in association with modulation of apoD levels in the APP-PS1 mouse brain, we went on to assess potential alterations in the APP processing pathway that could contribute to these changes. APP is sequentially cleaved by β- and γ-secretases to generate Aβ peptides of 39 to 42 amino acids, or it may undergo processing via the α-secretase pathway which is non-amyloidogenic as the α-cleavage occurs in the middle of the Aβ sequence and thereby precludes Aβ generation (De Strooper et al., 2010; Kang et al., 1987). During these proteolytic steps, membrane associated APP C-terminal fragments (CTFs) are generated that, along with an analysis of full length APP, can be used as a *de facto* measure of changes in the rate of APP proteolytic processing in the brain. The major APP CTFs formed result from: the α-cleavage, referred to as the "C83" CTF; the β-(BACE1)-cleavage, referred to as the "C99" CTF; and, at lower levels, the γ-secretase products of both C83 and C99 cleavage, referred to as the APP intracellular domain (AICD) fragment. The major APP CTF fragments used for quantification in the present study have an apparent MW of 9 kDa and 12 kDa, consistent with C83 and C99, respectively. The western blot bands we used for quantification are thus outlined on the full-length western blots included as supplementary data (Suppl. Fig. 1). Comparing the APP-PS1 and APP-PS1/DKO mice (Fig. 6A and 6C), the levels APP CTFs were found to be significantly increased (by 44%). This was associated with significantly increased (by ~2-fold) levels of BACE1 in the APP-PS1/DKO mice (Fig. 6B and 6C). Note that the increased

BACE1 in the APP-PS1/DKO mice was not likely to be due to the deletion of apoD *per se*, as BACE1 levels were essentially identical when WT and apoD null mice were compared (Suppl. Fig 2). Based on these results, we also assessed the same tissues for CTFs derived from BACE1-mediated cleavage of neuregulin-1 (NRG1), another well characterized BACE1 substrate (Fleck et al., 2012; Fleck et al., 2013; Hu et al., 2006). In this case, we detected a significant 27% increase in NRG1 CTFs in the APP-PS1/DKO mice (Fig. 6B and 6C).

Expression levels of these same proteins were also investigated in the brain homogenates derived from the APP-PS1/DTG mice. Intriguingly, and in contrast to the data derived from the APP-PS1/DKO mouse study, we found that the levels of APP CTFs were significantly reduced (by 40%) in the APP-PS1/DTG mice (Fig. 6D and 6F). Non-significant trends for decreased levels of BACE1 and NRG1 CTFs were also apparent (Fig. 6E and 6F). Although not statistically significant across all parameters, these data point towards an inverse association between apoD levels and BACE1 levels / activity in the brain.

To gain additional information regarding the potential modulation of BACE1 expression in the hippocampus, tissue sections were immunostained and the intensity of staining quantified. BACE1 appeared to be strongly expressed in the CA3 region of the hippocampus in all mice studied (Fig. 7). We also detected increased BACE1 staining in the vicinity of amyloid plaques as a general phenomenon across all mouse groups (typical examples are provided in Supplemental Figure 3). The quantitative analysis indicated hippocampal BACE1 levels were significantly increased by 25% in the APP-PS1/DKO mice compared to the APP-PS1 controls, whereas no change in BACE1 staining level was detected in the APP-PS1/DTG mice compared to the APP-PS1 controls (Fig. 7B). These data are in agreement with the western blot analysis of BACE1 (Fig. 6). As alterations in amyloid plaque pathology may be

associated with gliosis (Yan et al., 2009), we also assessed potential changes in glial markers GFAP (astrocytes) and Iba1 (microglia). An increase in hippocampal Iba1 (but not GFAP) staining was detected in APP-PS1/DKO mice compared to the APP-PS1 controls (Fig. 7), whereas no changes in either Iba1 or GFAP were detected in the APP-PS1/DTG mice compared to the APP-PS1 controls (Fig. 7). Colocalization immunohistochemical studies indicated that BACE1, GFAP and Iba1 staining were all clearly detected in the vicinity of amyloid plaques (Suppl. Fig. 3). It is therefore possible that at least part of the modulation of BACE1 levels is a response to the development of amyloid pathology. Consistent with this notion, there is evidence to suggest that a vicious cycle exists whereby Aβ and BACE1 both reciprocally up-regulate each others expression levels (Chami and Checler, 2012).

3.5. Impact of apoD modulation on markers of lipid peroxidation

Increased brain lipid peroxidation is associated with AD and is also a feature of AD mouse models, including the APP-PS1 line (Abdul et al., 2008; Markesbery and Carney, 1999). Based on the knowledge that apoD plays a significant role in protecting against lipid peroxidation in the brain (Ganfornina et al., 2008), we also assessed the mouse brain tissues for two markers of lipid peroxidation, HNE-modified proteins and F_2-isoprostanes. We previously reported that HNE-modified proteins in the range of ~56 kDa were positively associated with age in the human brain and inversely correlated with apoD expression (Kim et al., 2009), therefore similar protein markers were the focus in the present study. Although trends consistent with a lipid antioxidant function of apoD were noted (Fig. 8), no statistically significant changes in the abovementioned lipid peroxidation markers were detected. Altered lipid oxidation status therefore does not appear to be a major contributing factor in the altered AD pathology we have described in association with brain apoD levels in the APP-PS1

mouse model herein. Furthermore, the significant changes in plaque pathology associated with altered apoD expression we report do not appear to significantly modify brain lipid oxidation status.

4. Discussion

ApoD is a 29 kDa glycoprotein member of the lipocalin family (Rassart et al., 2000). The apoD crystal structure reveals an eight-stranded antiparallel β-barrel flanked by an α-helix (Eichinger et al., 2007). The β-barrel encloses a conically shaped hydrophobic cavity referred to as the apoD ligand binding pocket. Early studies suggested that apoD binds a range of lipids including arachidonic acid (AA), cholesterol and several steroids (Dilley et al., 1990; Lea, 1988; Morais Cabral et al., 1995; Pearlman et al., 1973). More recent studies indicate that binding of lipids in the apoD binding pocket is in fact quite specific (Eichinger et al., 2007; Oakley et al., 2012; Vogt and Skerra, 2001). Progesterone, AA and retinoic acid bind to the apoD binding pocket with high affinity whereas pregnenolone and specific eicosanoids (e.g. 12-HETE and 5,15-diHETE) also bind but with reduced affinity (Dilley et al., 1990; Lea, 1988; Morais Cabral et al., 1995; Ruiz et al., 2013). In addition to the binding pocket, apoD may also interact with lipids via a cluster of "exposed" hydrophobic residues residing in 3 of its extended loops (Eichinger et al., 2007; Oakley et al., 2012). These exposed residues generate a region of surface hydrophobicity close to the open end of the binding pocket that facilitates apoD association with high-density lipoprotein (HDL) particles and is also thought to permit insertion of apoD into cellular lipid membranes (Eichinger et al., 2007).

Several previous studies have shown that apoD levels are up-regulated in the AD brain (Bhatia et al., 2013; Terrisse et al., 1998; Thomas et al., 2003; Thomas et al., 2001), that there is a marked increase of neuronal apoD expression in AD (Desai et al., 2005; Kalman et al., 2000), and that apoD is found in amyloid plaques (Desai et al., 2005). Three studies have also reported associations between variations in the *APOD* gene and AD risk (Chen et al., 2008; Desai et al., 2003; Helisalmi et al., 2004). However, the direct role that apoD may play in modulating the course of AD has not been previously addressed. Our findings provide the first evidence that apoD expression levels do influence amyloid plaque pathology. It is intriguing that neuronal apoD expression is induced in human AD and in AD mouse models, yet a further increase, as achieved by transgenic neuronal expression in our current studies, is still able to significantly reduce amyloid plaque pathology. A similar outcome has also been reported in other studies using the same experimental approach to understand the function of proteins that may be involved in the regulation of AD pathology. For example, expression of the lipid transport protein ATP-binding cassette transporter A1 (ABCA1) is increased in the brain in human AD and AD mouse models (Kim et al., 2010), yet transgenic expression of ABCA1 in AD mice significantly reduces plaque pathology (Wahrle et al., 2008). It may be that for apoD, and other "protective" proteins like ABCA1, the homeostatic increase in protein expression is only partially protective, or is protective only later in the disease process when the up-regulation is stimulated in response to pathogenic stimuli. In contrast, transgenic expression of the protective protein could provide optimal protection through all stages of life and AD development, thus resulting in greater therapeutic efficacy.

Loss-of-function Drosophila mutants for the apoD homolog glial lazarillo (GLaz) were more sensitive to oxidative stress and contained higher concentrations of lipid peroxidation products; suggesting a function for apoD/GLaz in lipid peroxide (L-OOH) scavenging

(Sanchez et al., 2006). In agreement with this, over-expression of GLaz in transgenic Drosophila lines resulted in an increased resistance to oxidative stress, a 29% extension in lifespan and protection against hyperoxia-induced behavioural decline (Walker et al., 2006). In addition, expression of human apoD reduced the accumulation of aldehydic end-products of lipid peroxidation in old flies (Muffat et al., 2008). Similarly, the expression of human apoD in mouse neurons provided protection against paraquat-induced brain lipid peroxidation (Ganfornina et al., 2008). Since apoD provides lipid antioxidant protection in the brain (Ganfornina et al., 2008), one plausible mechanistic explanation could be due to the secondary regulation of Aβ production by brain lipid oxidation products. Previous studies have shown that oxidative stress and the products of lipid peroxidation, HNE in particular, up-regulate the expression of BACE1 leading to increased neuronal Aβ production (Paola et al., 2000; Tamagno et al., 2005). This would be consistent with the increase in BACE1 protein levels we observed in the APP-PS1/DKO mice as compared to their APP-PS1 littermates (Fig. 6). Although the converse (i.e. reduced BACE1) was not observed in the APP-PS1/DTG experiment, a decrease in APP CTFs including the BACE1 product (C99) was detected (Fig. 6). This provides initial evidence that the modulation of Aβ pathology by apoD may be mediated by BACE1. The precise mechanisms by which apoD modulates AD pathology remain to be resolved and, based on our current findings, this is an area that appears to warrant further investigation.

One limitation in our study is that we have not assessed additional groups of animals at earlier times points. Such future studies might reveal if BACE1 modulation plays a role in the earlier stage during development of AD pathology. Also related to this, at the time of animal cull at 11 months (a time chosen to ensure reasonable plaque load was present in all APP-PS1 mice), we detected only non-significant trends in HNE and F_2-isoprostane markers of lipid

peroxidation (Fig. 8). It is possible that with advancing stages of plaque pathology, a response to the predicted oxidativestresscanbemountedthatissufficientto“normalise”the lipid oxidative damage. We have shown previously in studies of post-mortem human brain that there is a coordinated up-regulation of apoD and additional antioxidant enzymes (superoxide dismutase 1 and glutathione peroxidase 3) associated with aging and increased levels of HNE-modified proteins (Kim et al., 2009). Follow up studies that focus on early time points of amyloid pathology development in these mice may add additional mechanistic insights.

ApoD may also regulate AD pathology via modulation of eicosanoids such as 5s-, 12s- and 15s-hydroperoxyeicosatetraenoic acids (HpETEs) that play a key role in brain inflammatory pathways (Phillis et al., 2006), and have been shown to be regulated by apoD *in vitro* (Bhatia et al., 2012; Oakley et al., 2012). Altered eicosanoid metabolism would be predicted to have significant impact on neuronal signalling and neuroinflammation in the AD context (Sanchez-Mejia and Mucke, 2010). Furthermore, pro-inflammatory conditions induced by lipopolysaccharide (LPS) have been shown to increase apoD expression in a time- and dose-dependent manner and the elements in the apoD promoter responsible (NF-κB, AP-1 and APRE-3) were confirmed to all be involved in the inflammatory response (Do Carmo et al., 2007). ApoD may also have an impact on the inflammatory pathways associated with AD pathology via regulation of specific cytokines. Previous studies in the Thy-1/ApoD (DTG) mice indicate that apoD protects against viral encephalitis by reducing both TNFα and IL1β expression and increasing IL6 expression (Do Carmo et al., 2008). This could potentially tie in with the concept regarding modulation of eicosanoid metabolism by apoD, as DTG mice have reduced phospholipase-A_2 (PLA2) activity in the brain (Do Carmo et al., 2008). Based on the facts that: (i), PLA2 is required to release arachidonic acid form phospholipids to

provide substrates for bioactive eicosanoids (Sanchez-Mejia and Mucke, 2010); (ii), PLA2 is up-regulated by TNFα and IL1β (Adibhatla and Hatcher, 2007); (iii), that inflammation promotes Aβ production and exacerbates amyloid plaque pathology (Sastre et al., 2003; Sastre et al., 2008; Yamamoto et al., 2007), it is reasonable to expect that apoD may regulate AD progression via such anti-inflammatory processes. In a preliminary screen, however, we did not detect changes in cortical levels of TNFα or ILβ in either the APP-PS1/DKO or APP-PS1/DTG mice compared to their APP-PS1 littermates (H. Li, S. Sanz Muñoz and B. Garner, unpublished data). Interestingly, both of the proposed mechanisms by which apoD may regulate amyloid plaque pathology (i.e. oxidative stress and inflammation) intersect at the BACE1 nexus (Chami and Checler, 2012).

In summary, the current studies using both gene knockout and neuronal overexpression approaches provide clear evidence that apoD regulates amyloid plaque pathology in a mouse model of AD. The role that apoD plays in the regulation of lipid oxidative stress, and neuroinflammation and the impact this has on BACE1-dependent and -independent pathways contributing to AD pathology is an area that appears to warrant further study.

Disclosure statement

The authors declare that they have no competing interests.

Acknowledgements

This research was supported by the National Health and Medical Research Council (NHMRC) of Australia (Grant ID #1065982) awarded to TK and BG. TK and BG are

supported by a NHMRC Research Fellowships (Grant ID #1045643 and #630445, respectively).

References

Abbott S.K., Jenner A.M., Mitchell T.W., Brown S.H., Halliday G.M., Garner B., 2013. An improved high-throughput lipid extraction method for the analysis of human brain lipids. Lipids 48, 307-318

Abdul H.M., Sultana R., St Clair D.K., Markesbery W.R., Butterfield D.A., 2008. Oxidative damage in brain from human mutant APP/PS-1 double knock-in mice as a function of age. Free Radic Biol Med 45, 1420-1425

Adibhatla R.M., Hatcher J.F., 2007. Secretory phospholipase A2 IIA is up-regulated by TNF-alpha and IL-1alpha/beta after transient focal cerebral ischemia in rat. Brain Res 1134, 199-205

Bajo-Graneras R., Ganfornina M.D., Martin-Tejedor E., Sanchez D., 2011. Apolipoprotein D mediates autocrine protection of astrocytes and controls their reactivity level, contributing to the functional maintenance of paraquat-challenged dopaminergic systems. Glia 59, 1551-1566

Bajo-Graneras R., Sanchez D., Gutierrez G., Gonzalez C., Do Carmo S., Rassart E., Ganfornina M.D., 2011. Apolipoprotein D alters the early transcriptional response to oxidative stress in the adult cerebellum. J Neurochem 117, 949-960

Bhatia S., Jenner A.M., Li H., Ruberu K., Spiro A.S., et al., 2013. Increased apolipoprotein D dimer formation in Alzheimer's disease hippocampus is associated with lipid conjugated diene levels. J Alzheimers Dis 35, 475-486

Bhatia S., Knoch B., Wong J., Kim W.S., Else P.L., Oakley A.J., Garner B., 2012. Selective reduction of hydroperoxyeicosatetraenoic acids to their hydroxy derivatives by apolipoprotein-D: Implications for lipid antioxidant activity and Alzheimer's disease. Biochem J 442, 713-721

Borchelt D.R., Davis J., Fischer M., Lee M.K., Slunt H.H., et al., 1996. A vector for expressing foreign genes in the brains and hearts of transgenic mice. Genet Anal 13, 159-163

Chami L., Checler F., 2012. BACE1 is at the crossroad of a toxic vicious cycle involving cellular stress and beta-amyloid production in Alzheimer's disease. Mol Neurodegener 7, 52

Chen Y., Jia L., Wei C., Wang F., Lv H., Jia J., 2008. Association between polymorphisms in the apolipoprotein D gene and sporadic Alzheimer's disease. Brain Res 1233, 196-202

Cheng D., Low J.K., Logge W., Garner B., Karl T., 2013. Novel behavioural characteristics of female APP/PS1DeltaE9 double transgenic mice. Behav Brain Res 260C, 111-118

Cristiano F., de Haan J.B., Iannello R.C., Kola I., 1995. Changes in the levels of enzymes which modulate the antioxidant balance occur during aging and correlate with cellular damage. Mech Ageing Dev 80, 93-105

Dassati S., Waldner A., Schweigreiter R., 2014. Apolipoprotein D takes center stage in the stress response of the aging and degenerative brain. Neurobiol Aging 35, 1632-1642

De Strooper B., Vassar R., Golde T., 2010. The secretases: enzymes with therapeutic potential in Alzheimer disease. Nat Rev Neurol 6, 99-107

Desai P.P., Hendrie H.C., Evans R.M., Murrell J.R., DeKosky S.T., Kamboh M.I., 2003. Genetic variation in apolipoprotein D affects the risk of Alzheimer disease in African-Americans. Am J Med Genet B Neuropsychiatr Genet 116B, 98-101

Desai P.P., Ikonomovic M.D., Abrahamson E.E., Hamilton R.L., Isanski B.A., Hope C.E., Klunk W.E., DeKosky S.T., Kamboh M.I., 2005. Apolipoprotein D is a component of compact but not diffuse amyloid-beta plaques in Alzheimer's disease temporal cortex. Neurobiol Dis 20, 574-582

Dilley W.G., Haagensen D.E., Cox C.E., Wells S.A., Jr., 1990. Immunologic and steroid binding properties of the GCDFP-24 protein isolated from human breast gross cystic disease fluid. Breast Cancer Res Treat 16, 253-260

Do Carmo S., Fournier D., Mounier C., Rassart E., 2009. Human apolipoprotein D overexpression in transgenic mice induces insulin resistance and alters lipid metabolism. Am J Physiol Endocrinol Metab 296, E802-811

Do Carmo S., Jacomy H., Talbot P.J., Rassart E., 2008. Neuroprotective effect of apolipoprotein D against human coronavirus OC43-induced encephalitis in mice. J Neurosci 28, 10330-10338

Do Carmo S., Levros L.C., Jr., Rassart E., 2007. Modulation of apolipoprotein D expression and translocation under specific stress conditions. Biochim Biophys Acta 1773, 954-969

Droge W., Schipper H.M., 2007. Oxidative stress and aberrant signaling in aging and cognitive decline. Aging Cell 6, 361-370

Eichinger A., Nasreen A., Kim H.J., Skerra A., 2007. Structural insight into the dual ligand specificity and mode of high density lipoprotein association of apolipoprotein D. J Biol Chem 282, 31068-31075

Elliott D.A., Weickert C.S., Garner B., 2010. Apolipoproteins in the brain – implications for neurological and psychiatric disorders. Clin Lipidol 5, 555-573

Fleck D., Garratt A.N., Haass C., Willem M., 2012. BACE1 dependent neuregulin processing: review. Curr Alzheimer Res 9, 178-183

Fleck D., van Bebber F., Colombo A., Galante C., Schwenk B.M., et al., 2013. Dual cleavage of neuregulin 1 type III by BACE1 and ADAM17 liberates its EGF-like domain and allows paracrine signaling. J Neurosci 33, 7856-7869

Franklin K.B.J., Paxinos G. (2007) *The Mouse Brain in Stereotaxic Coordinates*, (Third Edition) ed., Academic Press., New York, NY, USA

Ganfornina M.D., Do Carmo S., Lora J.M., Torres-Schumann S., Vogel M., et al., 2008. Apolipoprotein D is involved in the mechanisms regulating protection from oxidative stress. Aging Cell 7, 506-515

Garcia-Alloza M., Robbins E.M., Zhang-Nunes S.X., Purcell S.M., Betensky R.A., et al., 2006. Characterization of amyloid deposition in the APPswe/PS1dE9 mouse model of Alzheimer disease. Neurobiol Dis 24, 516-524

Ghosal K., Vogt D.L., Liang M., Shen Y., Lamb B.T., Pimplikar S.W., 2009. Alzheimer's disease-like pathological features in transgenic mice expressing the APP intracellular domain. Proc Natl Acad Sci U S A 106, 18367-18372

Gotz J., Ittner L.M., 2008. Animal models of Alzheimer's disease and frontotemporal dementia. Nat Rev Neurosci 9, 532-544

Helisalmi S., Hiltunen M., Vepsalainen S., Iivonen S., Corder E.H., Lehtovirta M., Mannermaa A., Koivisto A.M., Soininen H., 2004. Genetic variation in apolipoprotein D and Alzheimer's disease. J Neurol 251, 951-957

Higgins G.A., Jacobsen H., 2003. Transgenic mouse models of Alzheimer's disease: phenotype and application. Behav Pharmacol 14, 419-438

Hu X., Hicks C.W., He W., Wong P., Macklin W.B., Trapp B.D., Yan R., 2006. Bace1 modulates myelination in the central and peripheral nervous system. Nature neuroscience 9, 1520-1525

Jankowsky J.L., Fadale D.J., Anderson J., Xu G.M., Gonzales V., et al., 2004. Mutant presenilins specifically elevate the levels of the 42 residue beta-amyloid peptide in vivo: evidence for augmentation of a 42-specific gamma secretase. Hum Mol Genet 13, 159-170

Kalman J., McConathy W., Araoz C., Kasa P., Lacko A.G., 2000. Apolipoprotein D in the aging brain and in Alzheimer's dementia. Neurol Res 22, 330-336

Kang J., Lemaire H.G., Unterbeck A., Salbaum J.M., Masters C.L., Grzeschik K.H., Multhaup G., Beyreuther K., Muller-Hill B., 1987. The precursor of Alzheimer's disease amyloid A4 protein resembles a cell-surface receptor. Nature 325, 733-736

Kim W.S., Bhatia S., Elliott D.A., Agholme L., Kagedal K., McCann H., Halliday G.M., Barnham K.J., Garner B., 2010. Increased ATP-binding cassette transporter A1 expression in Alzheimer's disease hippocampal neurons. J Alzheimers Dis 21, 193-205

Kim W.S., Li H., Ruberu K., Chan S., Elliott D.A., Low J.K., Cheng D., Karl T., Garner B., 2013. Deletion of Abca7 increases cerebral amyloid-beta accumulation in the J20 mouse model of Alzheimer's disease. J Neurosci 33, 4387-4394

Kim W.S., Wong J., Weickert C.S., Webster M.J., Bahn S., Garner B., 2009. Apolipoprotein-D expression is increased during development and maturation of the human prefrontal cortex. J Neurochem 109, 1053-1066

Lagares A., Li H.Y., Zhou X.F., Avendano C., 2007. Primary sensory neuron addition in the adult rat trigeminal ganglion: evidence for neural crest glio-neuronal precursor maturation. J Neurosci 27, 7939-7953

Lea O.A., 1988. Binding properties of progesterone-binding Cyst protein, PBCP. Steroids 52, 337-338

Li H.Y., Say E.H., Zhou X.F., 2007. Isolation and characterization of neural crest progenitors from adult dorsal root ganglia. Stem cells 25, 2053-2065

Markesbery W.R., Carney J.M., 1999. Oxidative alterations in Alzheimer's disease. Brain Pathol 9, 133-146

Montine T.J., Quinn J., Kaye J., Morrow J.D., 2007. F(2)-isoprostanes as biomarkers of late-onset Alzheimer's disease. J Mol Neurosci 33, 114-119

Morais Cabral J.H., Atkins G.L., Sanchez L.M., Lopez-Boado Y.S., Lopez-Otin C., Sawyer L., 1995. Arachidonic acid binds to apolipoprotein D: implications for the protein's function. FEBS Lett 366, 53-56

Muffat J., Walker D.W., Benzer S., 2008. Human ApoD, an apolipoprotein up-regulated in neurodegenerative diseases, extends lifespan and increases stress resistance in Drosophila. Proc Natl Acad Sci U S A 105, 7088-7093

Oakley A.J., Bhatia S., Ecroyd H., Garner B., 2012. Molecular dynamics analysis of apolipoprotein-D-lipid hydroperoxide interactions: mechanism for selective oxidation of Met-93. PLoS One 7, e34057

Paola D., Domenicotti C., Nitti M., Vitali A., Borghi R., et al., 2000. Oxidative stress induces increase in intracellular amyloid beta-protein production and selective activation of betaI and betaII PKCs in NT2 cells. Biochem Biophys Res Commun 268, 642-646

Pearlman W.H., Gueriguian J.L., Sawyer M.E., 1973. A specific progesterone-binding component of human breast cyst fluid. J Biol Chem 248, 5736-5741

Phillis J.W., Horrocks L.A., Farooqui A.A., 2006. Cyclooxygenases, lipoxygenases, and epoxygenases in CNS: their role and involvement in neurological disorders. Brain Res Rev 52, 201-243

Rassart E., Bedirian A., Do Carmo S., Guinard O., Sirois J., Terrisse L., Milne R., 2000. Apolipoprotein D. Biochim Biophys Acta 1482, 185-198

Ruiz M., Sanchez D., Correnti C., Strong R.K., Ganfornina M.D., 2013. Lipid-binding properties of human ApoD and Lazarillo-related lipocalins: functional implications for cell differentiation. FEBS J 280, 3928-3943

Sanchez D., Lopez-Arias B., Torroja L., Canal I., Wang X., Bastiani M.J., Ganfornina M.D., 2006. Loss of glial lazarillo, a homolog of apolipoprotein D, reduces lifespan and stress resistance in Drosophila. Curr Biol 16, 680-686

Sanchez-Mejia R.O., Mucke L., 2010. Phospholipase A2 and arachidonic acid in Alzheimer's disease. Biochim Biophys Acta 1801, 784-790

Sastre M., Dewachter I., Landreth G.E., Willson T.M., Klockgether T., van Leuven F., Heneka M.T., 2003. Nonsteroidal anti-inflammatory drugs and peroxisome proliferator-activated receptor-gamma agonists modulate immunostimulated processing of amyloid precursor protein through regulation of beta-secretase. J Neurosci 23, 9796-9804

Sastre M., Walter J., Gentleman S.M., 2008. Interactions between APP secretases and inflammatory mediators. J Neuroinflammation 5, 25

Sayre L.M., Zelasko D.A., Harris P.L., Perry G., Salomon R.G., Smith M.A., 1997. 4-Hydroxynonenal-derived advanced lipid peroxidation end products are increased in Alzheimer's disease. J Neurochem 68, 2092-2097

Schuessel K., Schafer S., Bayer T.A., Czech C., Pradier L., Muller-Spahn F., Muller W.E., Eckert A., 2005. Impaired Cu/Zn-SOD activity contributes to increased oxidative damage in APP transgenic mice. Neurobiol Dis 18, 89-99

Tamagno E., Parola M., Bardini P., Piccini A., Borghi R., et al., 2005. Beta-site APP cleaving enzyme up-regulation induced by 4-hydroxynonenal is mediated by stress-activated protein kinases pathways. J Neurochem 92, 628-636

Terrisse L., Poirier J., Bertrand P., Merched A., Visvikis S., Siest G., Milne R., Rassart E., 1998. Increased levels of apolipoprotein D in cerebrospinal fluid and hippocampus of Alzheimer's patients. J Neurochem 71, 1643-1650

Terrisse L., Seguin D., Bertrand P., Poirier J., Milne R., Rassart E., 1999. Modulation of apolipoprotein D and apolipoprotein E expression in rat hippocampus after entorhinal cortex lesion. Brain Res Mol Brain Res 70, 26-35

Thomas E.A., Laws S.M., Sutcliffe J.G., Harper C., Dean B., et al., 2003. Apolipoprotein D levels are elevated in prefrontal cortex of subjects with Alzheimer's disease: no relation to apolipoprotein E expression or genotype. Biol Psychiatry 54, 136-141

Thomas E.A., Sautkulis L.N., Criado J.R., Games D., Sutcliffe J.G., 2001. Apolipoprotein D mRNA expression is elevated in PDAPP transgenic mice. J Neurochem 79, 1059-1064

Vogt M., Skerra A., 2001. Bacterially produced apolipoprotein D binds progesterone and arachidonic acid, but not bilirubin or E-3M2H. J Mol Recognit 14, 79-86

Wahrle S.E., Jiang H., Parsadanian M., Kim J., Li A., et al., 2008. Overexpression of ABCA1 reduces amyloid deposition in the PDAPP mouse model of Alzheimer disease. J Clin Invest 118, 671-682

Walker D.W., Muffat J., Rundel C., Benzer S., 2006. Overexpression of a Drosophila homolog of apolipoprotein D leads to increased stress resistance and extended lifespan. Curr Biol 16, 674-679

Wang J., Tanila H., Puolivali J., Kadish I., van Groen T., 2003. Gender differences in the amount and deposition of amyloid beta in APPswe and PS1 double transgenic mice. Neurobiol Dis 14, 318-327

Yamamoto M., Kiyota T., Horiba M., Buescher J.L., Walsh S.M., Gendelman H.E., Ikezu T., 2007. Interferon-gamma and tumor necrosis factor-alpha regulate amyloid-beta plaque deposition and beta-secretase expression in Swedish mutant APP transgenic mice. Am J Pathol 170, 680-692

Yan P., Bero A.W., Cirrito J.R., Xiao Q., Hu X., Wang Y., Gonzales E., Holtzman D.M., Lee J.M., 2009. Characterizing the appearance and growth of amyloid plaques in APP/PS1 mice. J Neurosci 29, 10706-10714

FIGURE LEGENDS

Fig. 1. Generation of APP-PS1/DKO and APP-PS1/DTG mice. APP-PS1/DKO mice and APP-PS1/DTG mice that either lack apoD or express human apoD in neurons, respectively, were generated as described in the "Materials and Methods" section. Cortical samples were assessed for mouse apoD mRNA (A) and human apoD mRNA (B) with each compared to the appropriate APP-PS1 littermate control mice (A, B). ApoD and apoE protein levels were assessed by western blotting and β-actin was used as a loading control (C, D). Relative protein and mRNA levels (where appropriate) were quantified using optical density of the scanned gels/blots (E, F). Representative samples are shown in the gels/blots. Quantitative data are means of 7 to 9 samples with the SE shown by the error bars. * $P < 0.05$; *** $P < 0.0001$; # trend, $P = 0.05$ to 0.06.

Fig. 2. ApoD immunohistochemical analysis in APP-PS1 and APP-PS1/DTG mice. Sagittal sections from wild type (WT), APP-PS1 and APP-PS1/DTG cortex were stained for apoD and NeuN to assess the extent of neuronal apoD localization. ApoD staining intensity was assessed using Image J software and the data expressed relative to the WT mice that were assigned an arbitrary relative plaque value of 1.0 (C). The white arrows indicate non-neuronal staining. Quantitative data are means of 3 to 4 samples with the SE shown by the error bars. ** $P < 0.05$ (for comparison of APP-PS1 and APP-PS1/DTG apoD staining). Scalebarin"F"=200μm.Scalebarin"I"=20μm.

Fig. 3. Impact of apoD loss on amyloid plaque pathology in APP-PS1 mice. Sagittal sections from APP-PS1 and APP-PS1/DKO mice were stained with 6E10 (A) or ThS (B) to assess amyloid plaque load. The area fraction of the hippocampal and cortical regions

occupied by plaques was calculated using Image J software and the data expressed as plaque levels relative to the APP/PS1 mice that were assigned an arbitrary relative plaque value of 1.0 (C-D). Grey bars, APP-PS1 group; black bars, APP-PS1/DKO group. Scale bars = 500 μm. All quantitative data are expressed as mean ± SE (represented by the error bars). * $P < 0.05$, ** $P < 0.01$.

Fig. 4. Impact of apoD modulation on soluble and insoluble Aβ species. Quantification of $A\beta_{40}$ and $A\beta_{42}$ levels in APP-PS1/DKO and APP-PS1/DTG hippocampal homogenates, relative to their appropriate APP-PS1 control mouse groups, was assessed by ELISA. For all samples, the "soluble" (A-B) and "insoluble" (guanidine HCl solubilised) Aβ species were quantified. Grey bars, APP-PS1 group; black bars, APP-PS1/DKO (DKO) or APP-PS1/DTG (DTG) group, as indicated. Scale bars = 500 μm. All quantitative data are expressed as mean ± SE (represented by the error bars). * $P < 0.05$, ** $P < 0.01$, $^{\#}$ $P = 0.08$ (non-significant trend).

Fig. 5. Impact of transgenic neuronal expression of human apoD on amyloid plaque pathology in APP-PS1 mice. Sagittal sections from APP-PS1 and APP-PS1/DTG mice were stained with 6E10 (A) or ThS (B) to assess amyloid plaque load. The area fraction of the hippocampal region occupied by plaques was calculated using Image J software and the data expressed as plaque levels relative to the APP/PS1 mice that were assigned an arbitrary relative plaque value of 1.0 (C). Grey bars, APP-PS1 group; black bars, APP-PS1/DTG group. Scale bars = 500 μm. All quantitative data are expressed as mean ± SE (represented by the error bars). * $P < 0.05$, ** $P < 0.01$.

Fig. 6. Impact of apoD modulation on APP processing. Hippocampal homogenates derived from APP-PS1/DKO, APP-PS1/DTG and their appropriate control APP-PS1 groups were probed for the proteins listed by western blotting (A, B, D, E). Representative blots (n = 4 to 5 samples for each group) are shown. β-Actin is used as a loading control. Integrated optical density for blots of all samples is shown (C, F). Grey bars, APP-PS1 group; black bars, APP-PS1/DKO or APP-PS1/DTG group. Levels are expressed relative to APP-PS1 mice and presented as mean ± SE. * $P < 0.05$, *** $P < 0.0001$. APP, amyloid precursor protein; CTFs, APP C-terminal fragments; BACE1, beta-site APP cleaving enzyme-1; NRG1 CTFs, neuregulin-1 C-terminal fragments. Note that consistent with previous data (Ghosal et al., 2009), the major APP CTFs are tentatively assigned as C99 (CTFβ , 12 kDa) and C83 (CTFα, 9.2 kDa). The identity of a third apparent APP CTF band at ~15 kDa is unknown and its levels were not used in the data presented (although inclusion of this band in the analysis did not alter the data). For quantification, the optical density of the two major APP CTF bands were measured together. Full-length western blots related to APP CTF proteolytic products are provided in Supplementary materials (Suppl. Fig. 1).

Fig. 7. Impact of apoD modulation on hippocampal BACE1, GFAP, and Iba1 levels assessed by immunohistochemistry. Sagittal sections from APP-PS1/DKO and APP-PS1/DTG mice and their appropriate control APP-PS1 groups were immunostained for BACE1, GFAP and Iba1 (A), and the staining intensity quantified using ImageJ software. The data are presented as protein levels relative to the APP/PS1 mice that were assigned an arbitrary relative value of 1.0 (B). Grey bars, APP-PS1 group; black bars, APP-PS1/DKO (DKO) or APP-PS1/DTG (DTG) group. Statistical differences are expressed relative to APP-PS1 control mice and data presented as mean ± SE, n = 4 to 5 sections per group. * $P < 0.05$. Scale bar = 500 μm.

Fig. 8. Impact of apoD modulation on markers of lipid oxidative stress. Brain homogenates derived from APP-PS1/DKO, APP-PS1/DTG and their appropriate control APP-PS1 groups were probed for the proteins modified by the lipid peroxidation aldehydic product 4-hydroxynonenal (HNE) by western blotting (A, B). Representative blots (n = 4 to 7 samples for each group) are shown. β-Actin is used as a loading control. Integrated optical density for blots of all samples is shown (C). Grey bars, APP-PS1 group; black bars, APP-PS1/DKO or APP-PS1/DTG group. Comparison of F_2-isoprostane levels in APP-PS1/DKO or APP-PS1/DTG groups and their appropriate control APP-PS1 groups. Lipids were extracted, the F_2-isoprostane fraction was purified by solid phase extraction and F_2-isoprostane PFBenzyl esters were prepared and derivatised with BSTFA and TMCS for analysis using GC-MS. The F_2-isoprostanes were quantified by comparison to internal standards. Data are expressed as pg F_2-isoprostane per μg of arachidonic acid (AA). Levels are expressed relative to APP-PS1 mice and presented as mean $\pm$ SE.

SUPPLEMENTARY FIGURE LEGENDS

Suppl. Fig. 1. Impact of apoD modulation on APP processing – full length western blots demonstrating position of APP CTFs. Hippocampal homogenates derived from APP-PS1/DKO, APP-PS1/DTG and their appropriate control APP-PS1 groups were probed for the APPandAPPproteolyticproducts.Theregionmarkedas"CTFs"representthepanelsthat are shown for APP CTFs in Fig. 6. Note that consistent with previous data (Ghosal et al., 2009), the major APP CTFs are tentatively assigned as C99 (CTFβ , 12 kDa) and C83 (CTFα, 9.2 kDa). The identity of a third apparent APP CTF band at ~15 kDa is unknown and its levels were not used in the data presented (although inclusion of this band in the analysis did not alter the data). For quantification, the optical density of the two major APP CTF bands were measured together (shown by the dashed red line boxes in the blots on the right hand side). APP, amyloid precursor protein; CTFs, APP C-terminal fragments.

Suppl. Fig. 2. Hippocampal BACE1 expression is not altered in apoD null mice. Hippocampal homogenates derived from wild type (WT) and apoD null ($apoD^{-/-}$) mice (in the absence of the APP-PS1 background) were probed for apoD, BACE1, and β -actin by western blotting. The representative blots indicate no change in BACE1 levels in either male of female $apoD^{-/-}$mice as compared to WT control mice.

Suppl. Fig. 3. Distribution pattern of hippocampal BACE1, GFAP and IBa1 with amyloid plaques by double-staining immunofluorescence. Sagittal sections from brains of APP-PS1/DKO mice were used for double-labelling with an Aβ antibody and a BACE1 antibody to demonstrate the distribution of BACE1 and its relationships with amyloid plaque (A). The confocal images demonstrate that BACE1 is localize around WO2-positive plaques

and in the CA3 region where the highest BACE1 level is detected. Staining for glial markers GFAP (astrocytes) and Iba1 (microglia) close to the hippocampal CA3 region also demonstrated a close association of these glial markers around WO2-positive plaques (B). Scale bar in“A”= 500 μ m,scalebarsin“B”= 100 μm.

Figure1

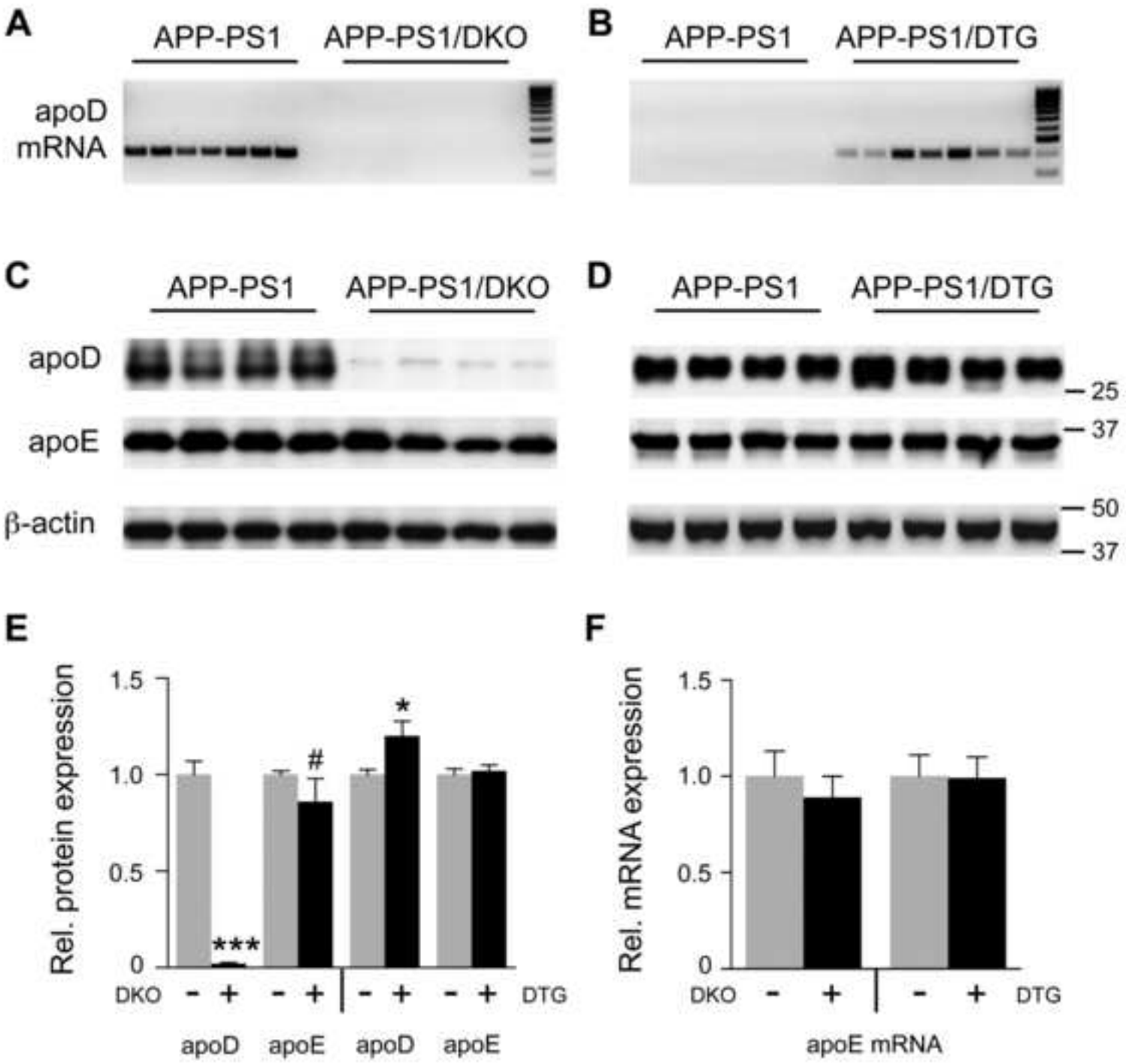
A
APP-PS1
APP-PS1/DKO
apoD
mRNA
B
APP-PS1
APP-PS1/DTG
C
APP-PS1
APP-PS1/DKO
apoD
apoE
β-actin
D
APP-PS1
APP-PS1/DTG
25
37
50
37
E
Rel. protein expression
1.5
1.0
0.5
0
***
#
*
DKO - + - + - + - + DTG
apoD apoE apoD apoE
F
Rel. mRNA expression
1.5
1.0
0.5
0
DKO - + - + DTG
apoE mRNA

Figure2

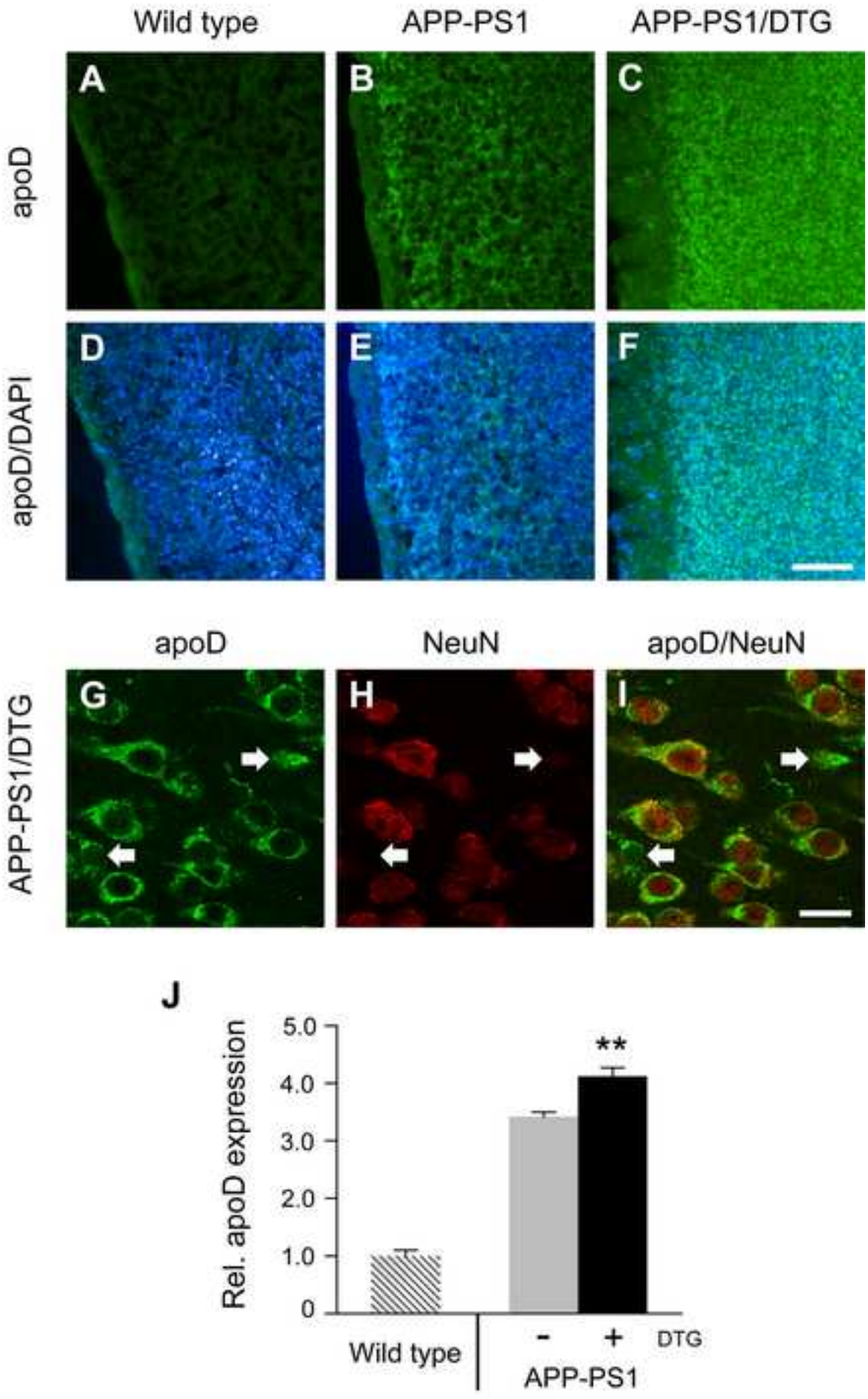
Wild type
APP-PS1
APP-PS1/DTG
apoD
apoD/DAPI
A
B
C
D
E
F
apoD
NeuN
apoD/NeuN
APP-PS1/DTG
G
H
I
J
Rel. apoD expression
5.0
4.0
3.0
2.0
1.0
0
**
Wild type
-
+
DTG
APP-PS1

Figure3

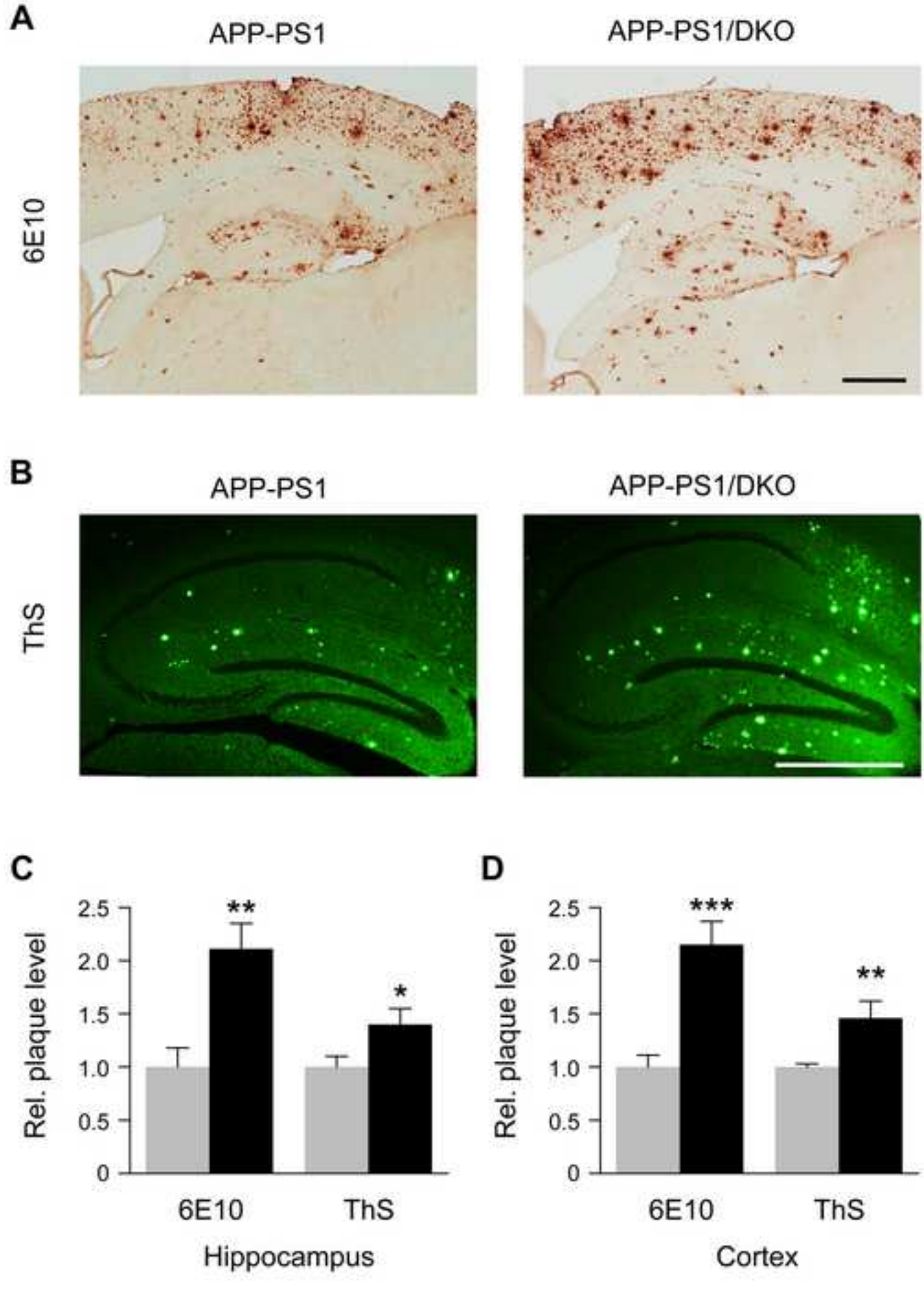
A
APP-PS1
APP-PS1/DKO
6E10
B
APP-PS1
APP-PS1/DKO
ThS
C
Rel. plaque level
2.5
2.0
1.5
1.0
0.5
0
**
*
6E10
ThS
Hippocampus
D
Rel. plaque level
2.5
2.0
1.5
1.0
0.5
0
***
**
6E10
ThS
Cortex

Figure4

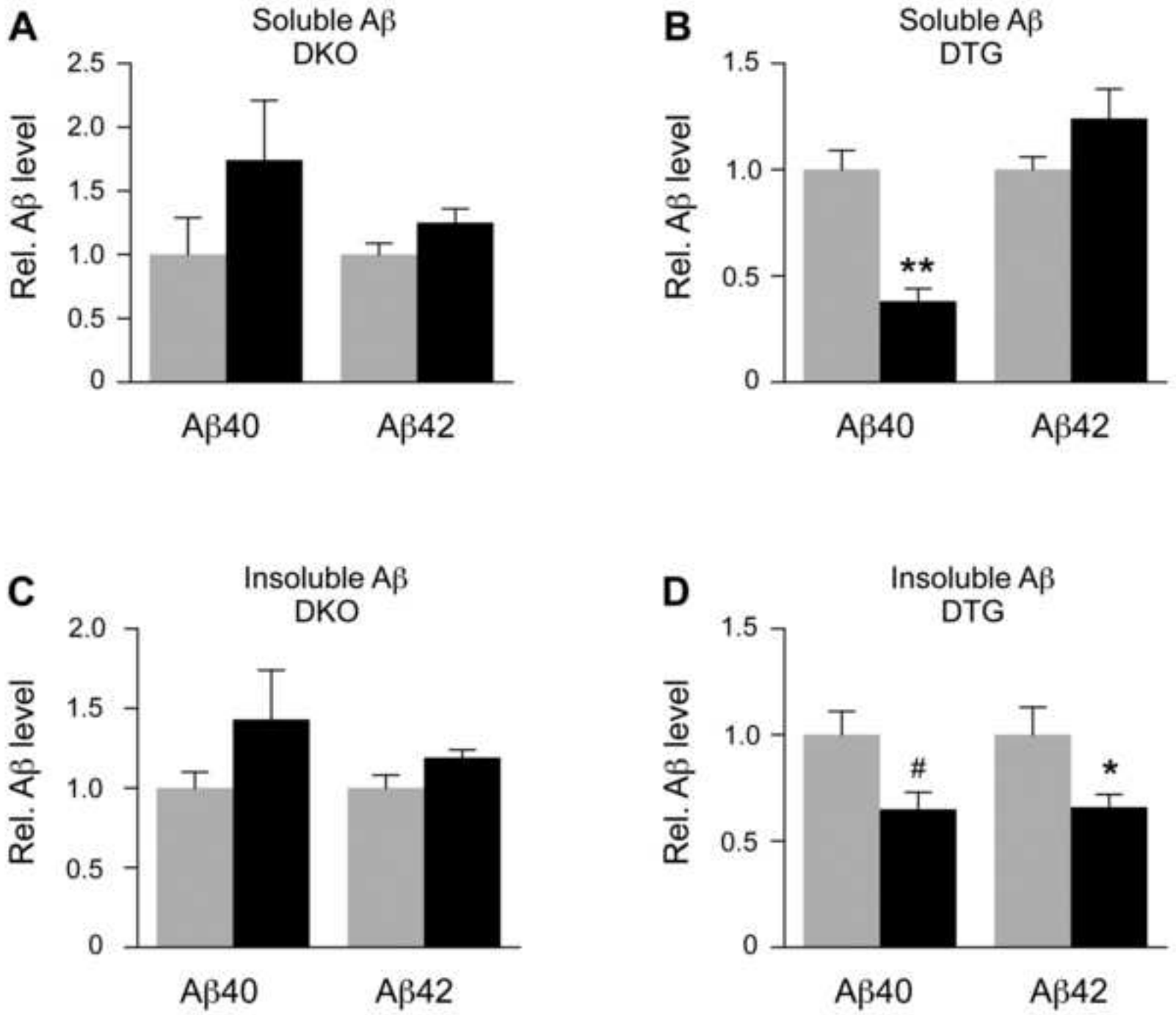
A
Soluble Aβ
DKO
Rel. Aβ level
2.5
2.0
1.5
1.0
0.5
0
Aβ40
Aβ42
B
Soluble Aβ
DTG
Rel. Aβ level
1.5
1.0
0.5
0
**
Aβ40
Aβ42
C
Insoluble Aβ
DKO
Rel. Aβ level
2.0
1.5
1.0
0.5
0
Aβ40
Aβ42
D
Insoluble Aβ
DTG
Rel. Aβ level
1.5
1.0
0.5
0
#
*
Aβ40
Aβ42

Figure5

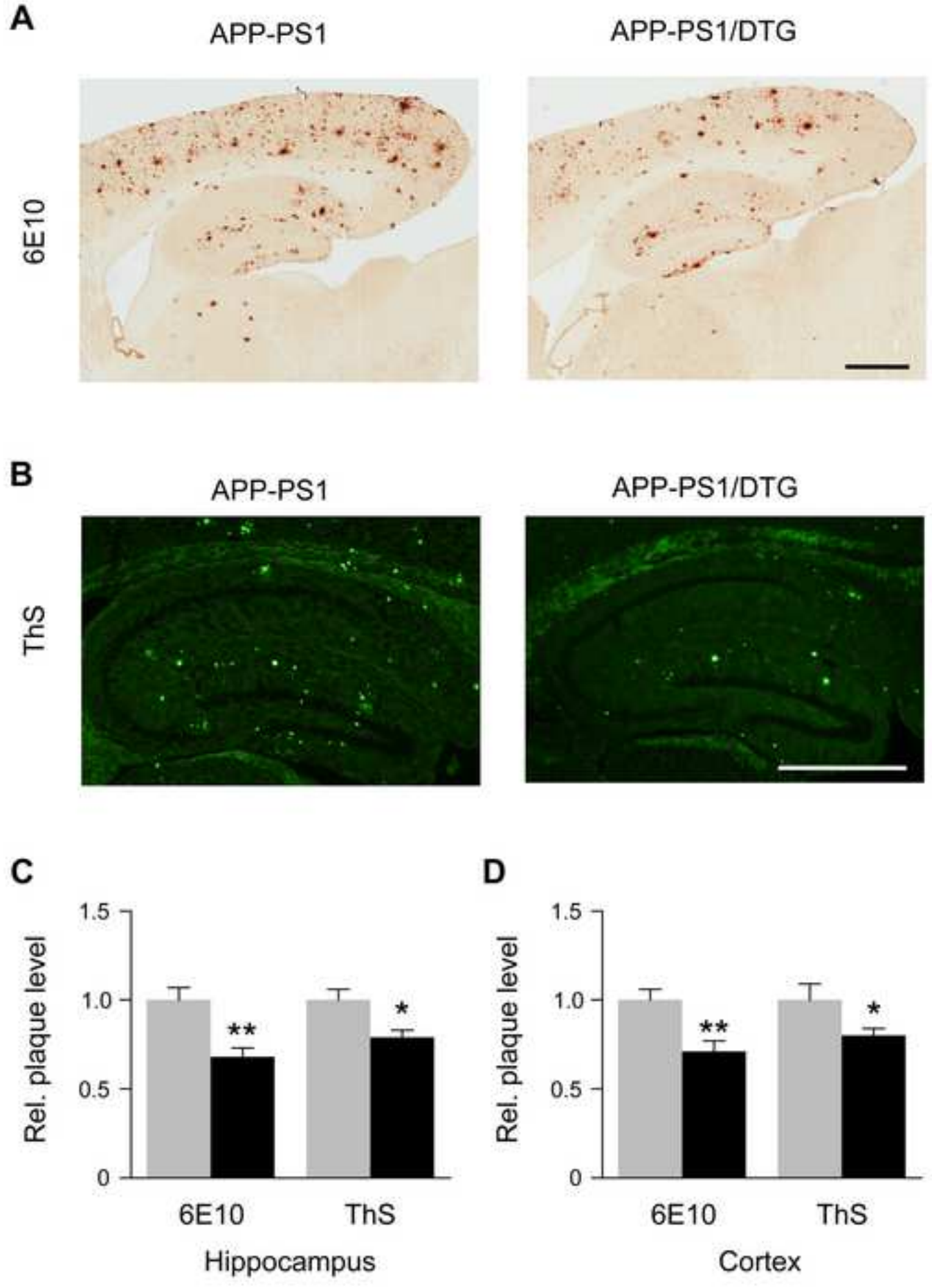
A
APP-PS1
APP-PS1/DTG
6E10
B
APP-PS1
APP-PS1/DTG
ThS
C
Rel. plaque level
1.5
1.0
0.5
0
**
*
6E10
ThS
Hippocampus
D
Rel. plaque level
1.5
1.0
0.5
0
**
*
6E10
ThS
Cortex

Figure6

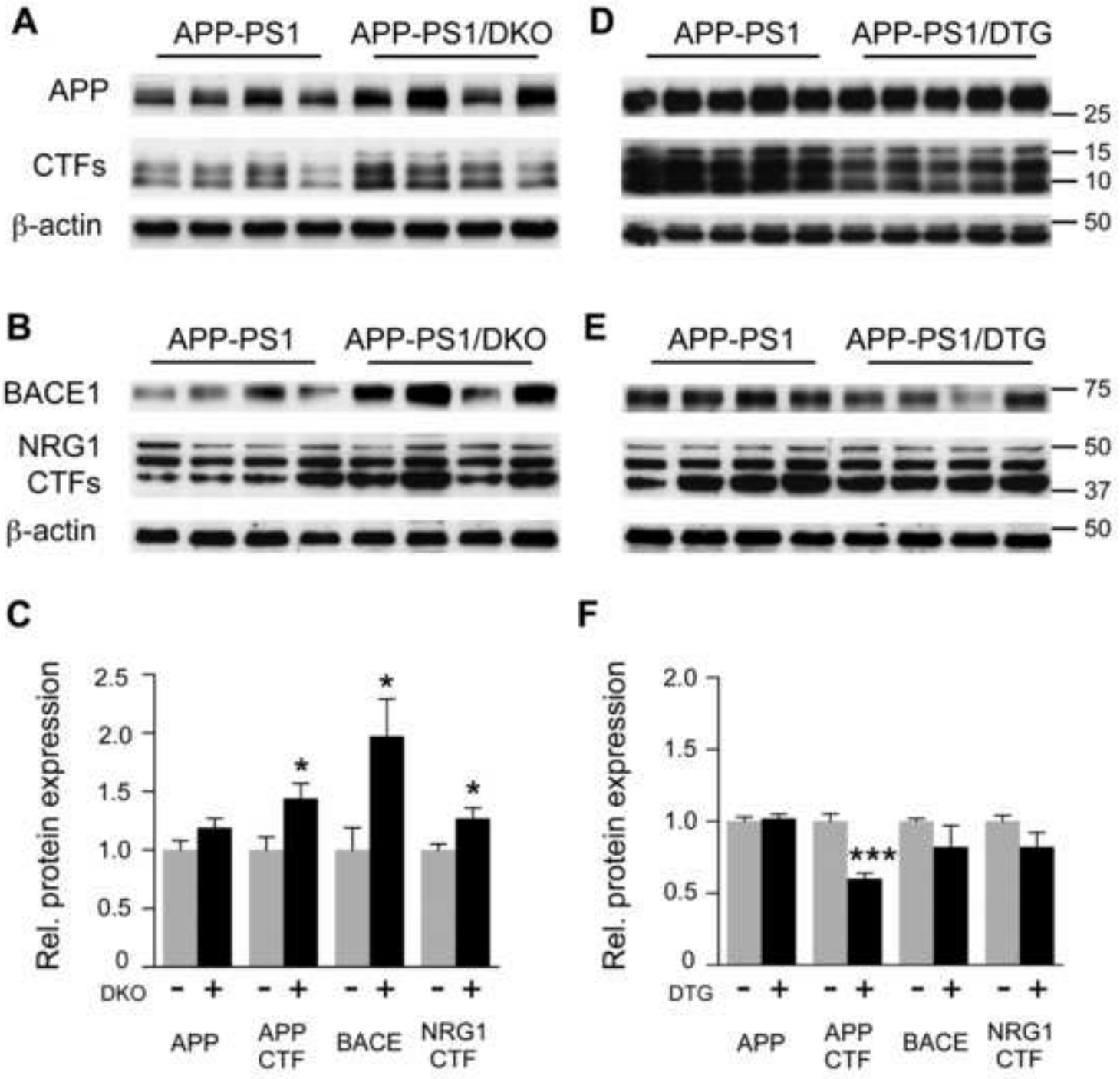
A
APP-PS1
APP-PS1/DKO
APP
CTFs
β-actin
D
APP-PS1
APP-PS1/DTG
25
15
10
50
B
APP-PS1
APP-PS1/DKO
BACE1
NRG1
CTFs
β-actin
E
APP-PS1
APP-PS1/DTG
75
50
37
50
C
Rel. protein expression
2.5
2.0
1.5
1.0
0.5
0
DKO - + - + - + - +
APP
APP CTF
BACE
NRG1 CTF
F
Rel. protein expression
2.0
1.5
1.0
0.5
0
DTG - + - + - + - +
APP
APP CTF
BACE
NRG1 CTF

Figure7

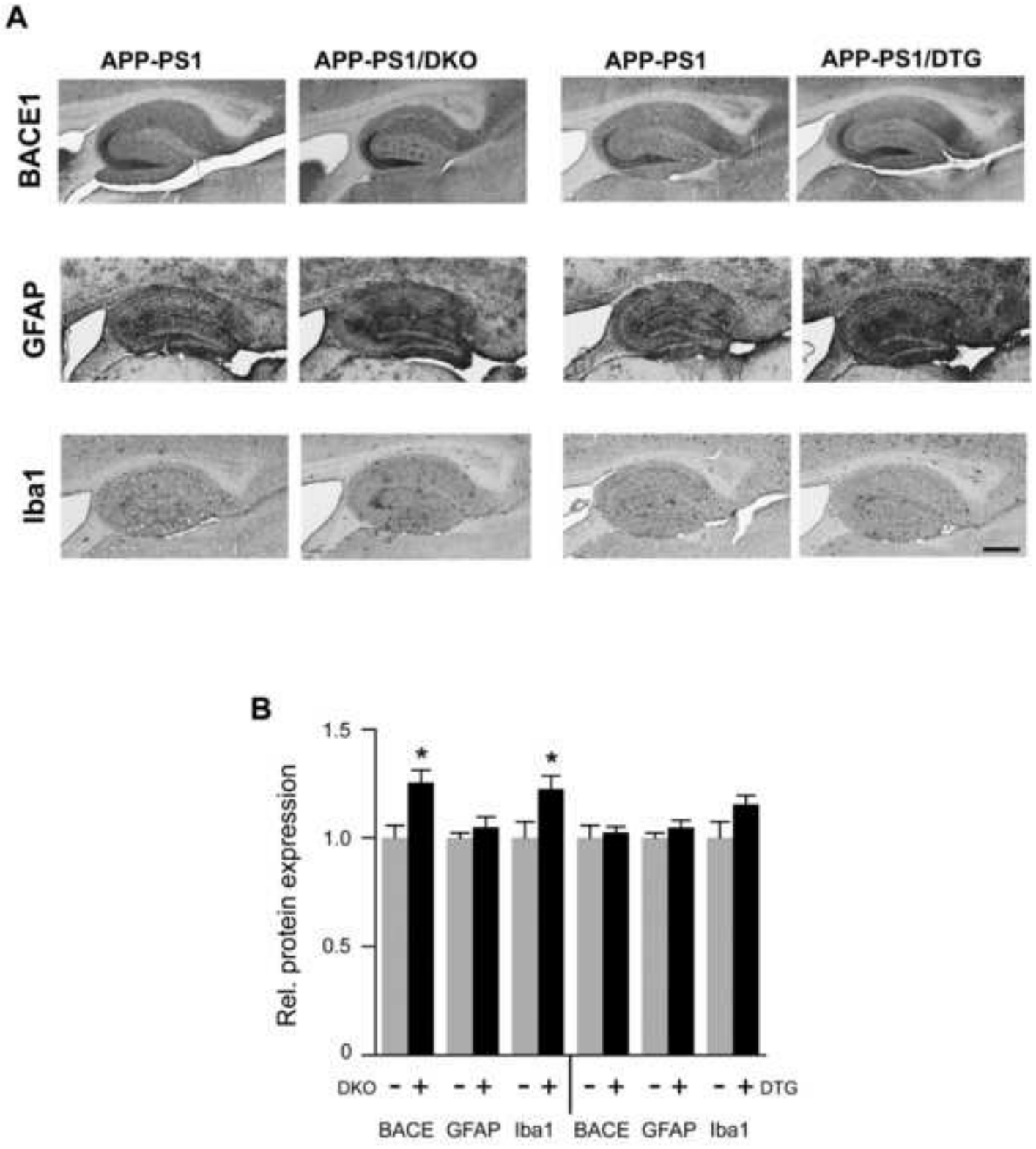
A
APP-PS1
APP-PS1/DKO
APP-PS1
APP-PS1/DTG
BACE1
GFAP
Iba1
B
Rel. protein expression
1.5
1.0
0.5
0
DKO - + - + - + - + - + - + DTG
BACE GFAP Iba1 BACE GFAP Iba1

Figure8

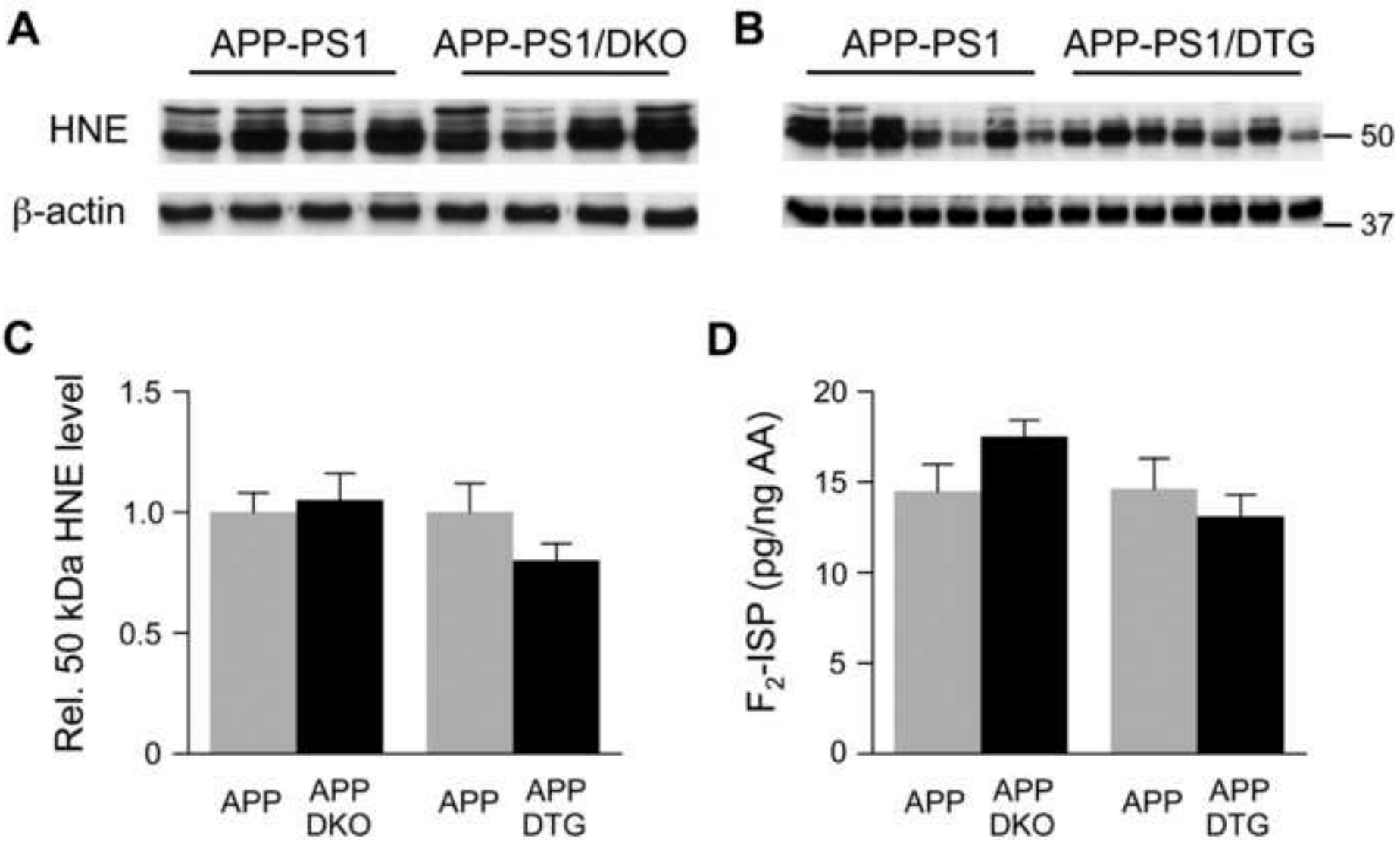
A
APP-PS1
APP-PS1/DKO
HNE
β-actin
B
APP-PS1
APP-PS1/DTG
50
37
C
Rel. 50 kDa HNE level
1.5
1.0
0.5
0
APP
APP DKO
APP
APP DTG
D
F2-ISP (pg/ng AA)
20
15
10
5
0
APP
APP DKO
APP
APP DTG

Supplemental Fig1

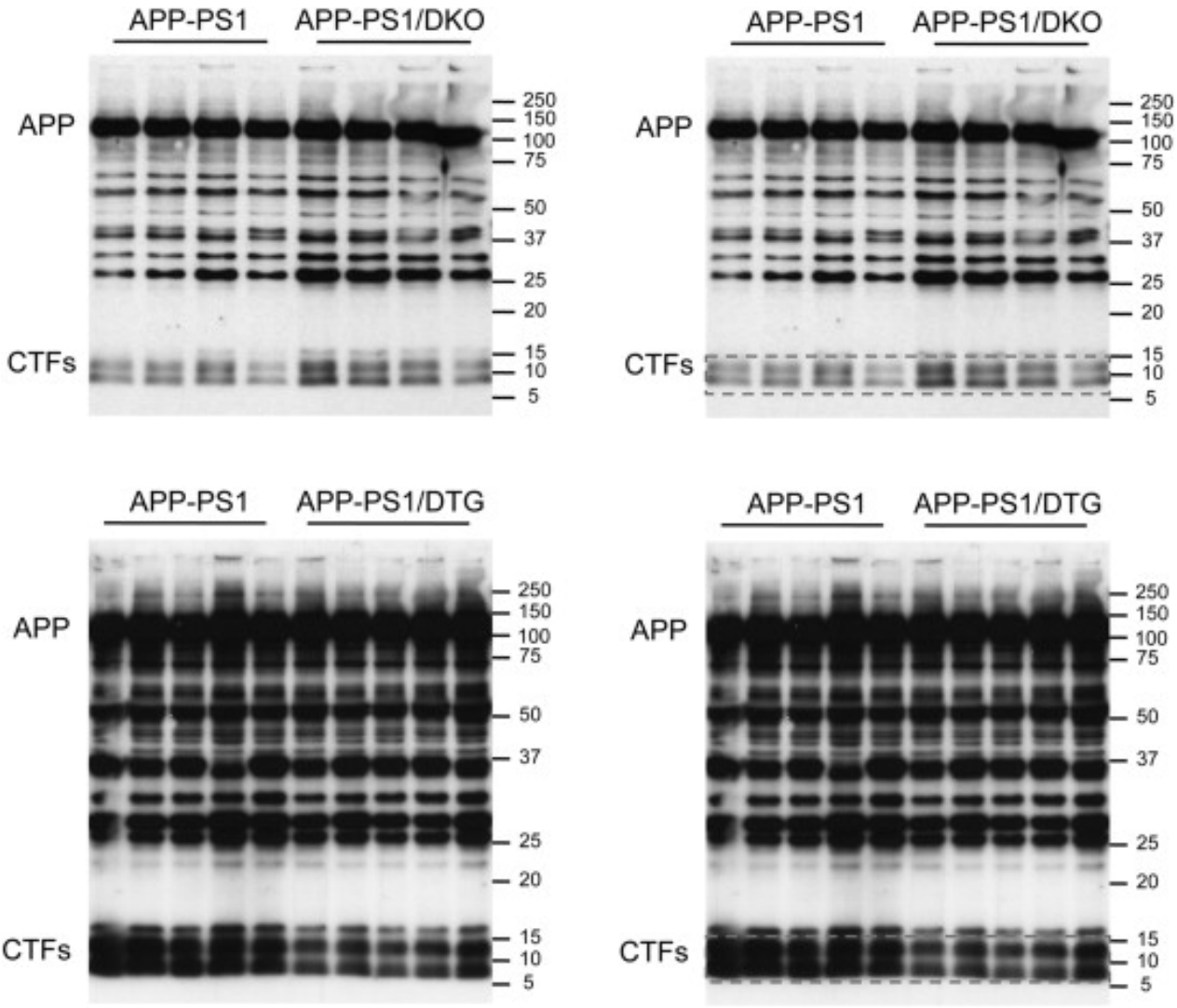

Supplemental Fig2

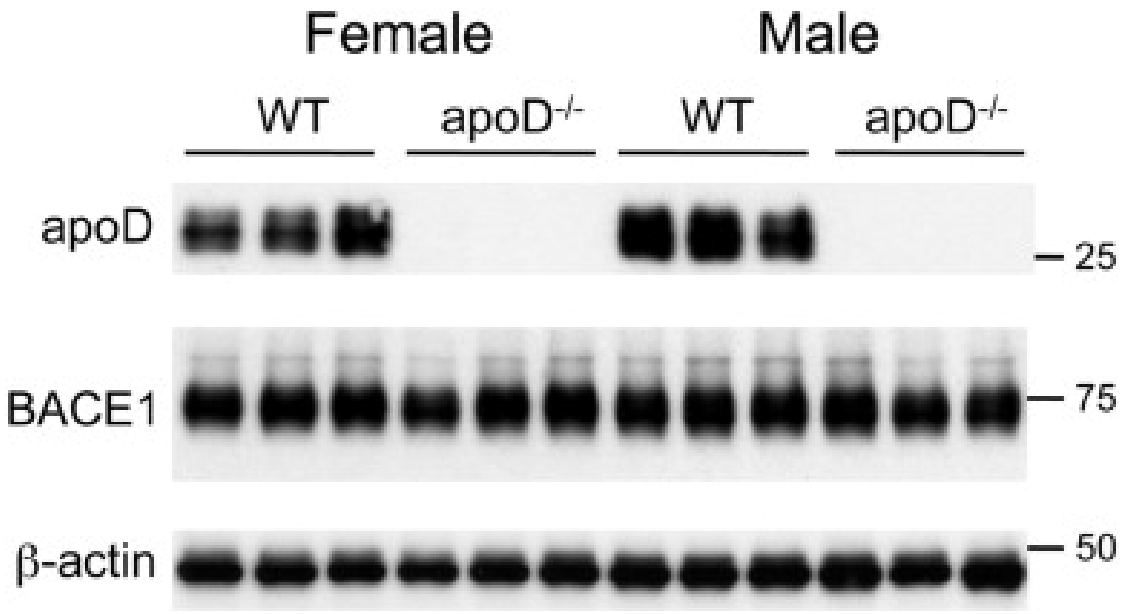

Supplemental Fig3

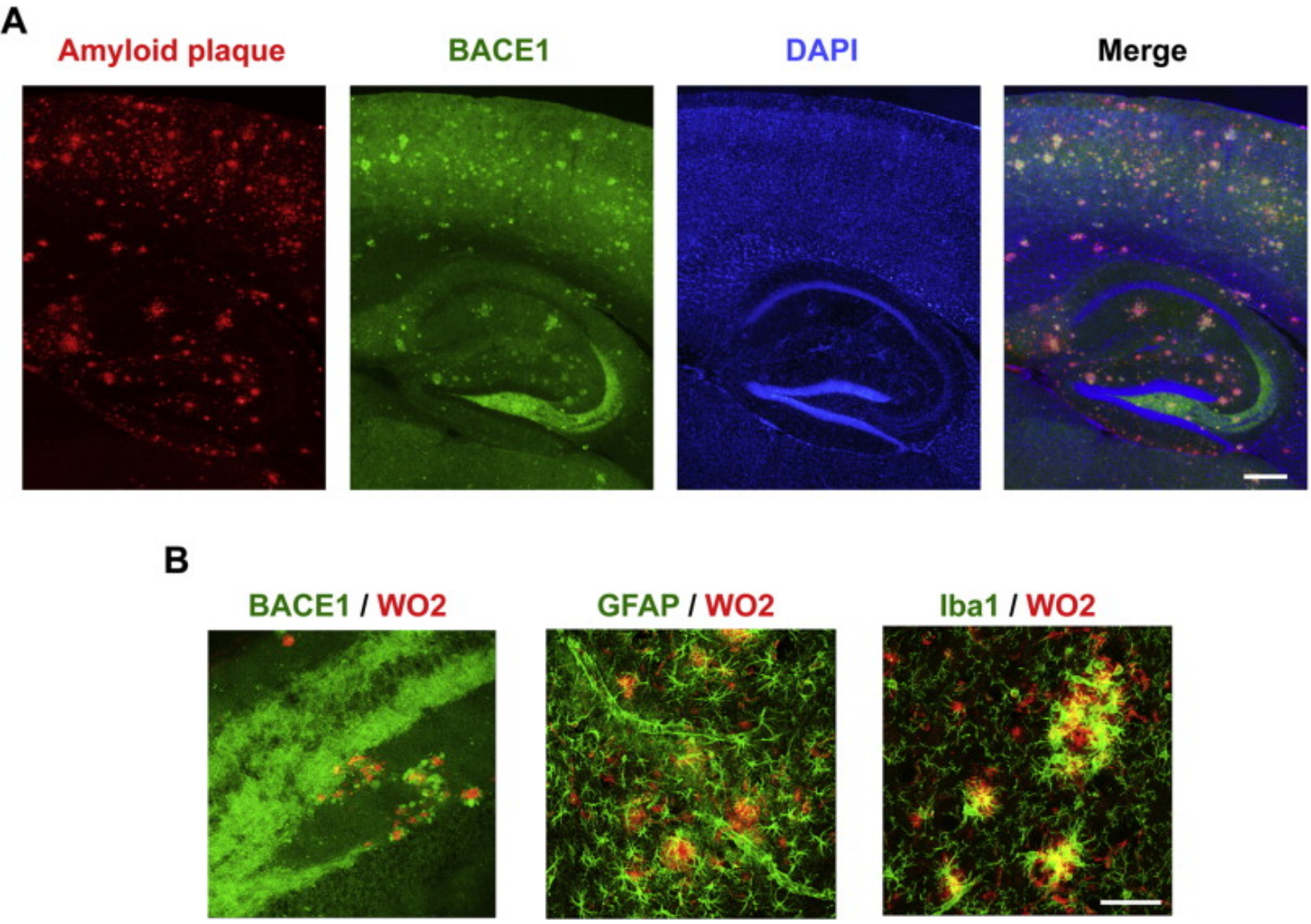

***Highlights (for review)**

Research highlights

- Brain apoD levels are increased with aging and Alzheimer's disease
- It was unclear if apoD modulates amyloid pathology in vivo
- ApoD deletion exacerbated amyloid pathology in the APP/PS1 mice
- Transgenic neuronal apoD expression reduced amyloid pathology in the APP/PS1 mice